

# Extremal Random Forests

Nicola Gnecco<sup>\*1</sup>, Edossa Merga Terefe<sup>\*1, 2</sup>, and Sebastian Engelke<sup>1</sup>

<sup>1</sup>Research Center for Statistics, University of Geneva, Switzerland

<sup>2</sup>Statistics Department, Hawassa University, Ethiopia

<sup>1</sup> {*nicola.gnecco, edossa.terefe, sebastian.engelke*} @unige.ch

February 1, 2022

## Abstract

Classical methods for quantile regression fail in cases where the quantile of interest is extreme and only few or no training data points exceed it. Asymptotic results from extreme value theory can be used to extrapolate beyond the range of the data, and several approaches exist that use linear regression, kernel methods or generalized additive models. Most of these methods break down if the predictor space has more than a few dimensions or if the regression function of extreme quantiles is complex. We propose a method for extreme quantile regression that combines the flexibility of random forests with the theory of extrapolation. Our extremal random forest (ERF) estimates the parameters of a generalized Pareto distribution, conditional on the predictor vector, by maximizing a local likelihood with weights extracted from a quantile random forest. Under certain assumptions, we show consistency of the estimated parameters. Furthermore, we penalize the shape parameter in this likelihood to regularize its variability in the predictor space. Simulation studies show that our ERF outperforms both classical quantile regression methods and existing regression approaches from extreme value theory. We apply our methodology to extreme quantile prediction for U.S. wage data.

*Keywords:* extreme quantiles; local likelihood estimation; quantile regression; random forests; threshold exceedances.

## 1 Introduction

Quantile regression is a well-established technique to model statistical quantities that go beyond the conditional expectation that is used for standard regression analysis ([Koenker and Bassett, 1978](#)).

---

<sup>\*</sup>Authors contributed equally.

This is particularly valuable in applications such as economics, survival analysis, medicine, and finance (Angrist et al., 2006; Yang, 1999; Heagerty and Pepe, 1999; Taylor, 1999; Yu et al., 2003), where one needs to model the heteroschedasticity of the response or conditional quantiles such as the median.

In this paper, we consider the problem of estimating high conditional quantiles of a response variable  $Y \in \mathbb{R}$  given a set of predictors  $X \in \mathbb{R}^p$  in large dimensions, an important task in risk assessment for rare events (Chernozhukov, 2005). For a fixed predictor value  $x$ , define  $Q_x(\tau)$  as the quantile at level  $\tau \in (0, 1)$  of the conditional distribution of  $Y \mid X = x$ . We are interested in the estimation of extreme quantiles where  $\tau \approx 1$  is close to one. This estimation problem exhibits two fundamental challenges that are illustrated in Figure 1, which shows a simulation similar to Athey et al. (2019, Figure 2). The predictor space has  $p = 40$  dimensions and only the first variable  $X_1$  has a signal corresponding to a scale shift in  $Y$ ; see Example 1 in Section 3.1 for details.

The first challenge in estimating  $Q_x(\tau)$  relates to the fact that for an extreme probability level, say  $\tau = 0.9995$  as in Figure 1, there are typically only few or no observations in the sample that exceed the corresponding conditional  $\tau$ -quantiles. Indeed, for a sample of size  $n$ , the expected number of exceedances above the conditional  $\tau$ -quantile is  $n(1 - \tau)$ , which becomes smaller than one if  $\tau > 1 - 1/n$ . Therefore, using an empirical estimator based on quantile loss leads to a large bias. A second challenge stems from the possibly high-dimensional predictor space  $\mathbb{R}^p$ , where there might be no training observations close to  $x$ ; note that the Figure 1 only shows the first of the 40 dimensions of  $X$ . Too simple regression models may then introduce additional bias.

The first challenge can be addressed by relying on tail approximations motivated by extreme value theory (e.g., de Haan and Ferreira, 2006), which allow the extrapolation to quantile levels beyond the range of the data. Such methods typically consider (transformations of) linear (Chernozhukov, 2005; Wang and Tsai, 2009; Wang et al., 2012; Wang and Li, 2013) functions, additive models (Chavez-Demoulin and Davison, 2005; Youngman, 2019), non-parametric regression (Beirlant et al., 2004; Martins-Filho et al., 2015) and local smoothing methods (Daouia et al., 2011; Gardes and Stupfler, 2019; Velthoen et al., 2019). However, these existing approaches are either not flexible enough to model complex response surfaces or do not scale well in higher dimensions  $p$  of the predictor space.

Regarding the second challenge, several quantile regression methods have been proposed in the statistical and machine learning literature that can cope with high-dimensional predictor spaces and complex regression surfaces (Taylor, 2000; Friedman, 2001). In particular, there exist several forest-based approaches for quantile regression (Meinshausen, 2006; Athey et al., 2019). These methods are based on (extensions of) the random forest originally developed by Breiman (2001) and can estimate flexible quantile regression functions. Compared to methods such as gradient boosting and neural networks, the main advantage of forest-based approaches is that they require little tuning and that their statistical properties are relatively well understood (Athey et al., 2019). Moreover, they scale well with the dimension of the predictor space as opposed to approaches based on generalized additive models (Koenker, 2011) and kernel-based methods (Yu and Jones, 1998). While these methods work well for estimation of quantiles inside the data range, such as  $\tau_0 = 0.8$  in Figure 1, their performance deteriorates for quantile estimation at extreme levels  $\tau \approx 1$  close to the upper endpoint of the response distribution.

In this paper, we bring together ideas from extreme value theory and forest-based regression methods to tackle the challenges of extreme quantile regression in predictor spaces with possibly high dimensions  $p$ . To extrapolate beyond the data range, we rely on the approximation by the generalized Pareto distribution (GPD) of the exceedances over an intermediate threshold; see the triangles in Figure 1. Under mild assumptions, the conditional quantile of  $Y$ , given  $X = x$ , at level  $\tau \approx 1$  can be approximated by (Balkema and de Haan, 1974; Pickands, 1975)

$$Q_x(\tau) \approx Q_x(\tau_0) + \frac{\sigma(x)}{\xi(x)} \left[ \left( \frac{1 - \tau}{1 - \tau_0} \right)^{-\xi(x)} - 1 \right], \quad (1.1)$$

where  $Q_x(\tau_0)$  is an intermediate quantile at level  $\tau_0 < \tau$  and the second term on the right-hand side is quantile function of the GPD indexed by the conditional scale  $\sigma(x) > 0$  and shape parameter  $\xi(x) \in \mathbb{R}$ . This includes responses with heavy tails ( $\xi(x) > 0$ ), light tails ( $\xi(x) = 0$ ) and with finite upper end points ( $\xi(x) < 0$ ). The intermediate quantile level  $\tau_0$  is chosen small enough such that the conditional quantiles  $Q_x(\tau_0)$  can be estimated by classical regression methods. At the same time, it should be large enough so that the approximation in (1.1) by the GPD is accurate.

In order to cope with complex response surfaces and high-dimensional predictor spaces, we rely on ideas from the random forest literature (Meinshausen, 2006; Athey et al., 2019). Our new extremal random forest (ERF) localizes the estimation of the GPD parameter vector  $\theta(x) = (\sigma(x), \xi(x))$  around the predictor value  $x$  using forest-based weights. Since only few extreme observations are typically available for training, the simple tuning of random forests turns out to be of great advantage. Under certain conditions, we show consistency of the ERF estimator  $\hat{\theta}(x)$  for the true conditional parameter vector  $\theta(x)$ . Since our loss function, namely the GPD log-likelihood, is non-convex, the proof strategy of Athey et al. (2019) cannot be used, and we rely on the theory of Newey (1991).

Our ERF algorithm combines the advantages of accurate tail extrapolation at levels  $\tau \approx 1$  with a flexible regression method that scales well with predictor dimension. In simulations, we show that ERF outperforms extreme value theory and quantile regression methods to estimate extreme quantiles. Moreover, it is competitive with the recent gradient boosting by Velthoen et al. (2021) and has the advantage of significantly easier tuning and the theoretical guarantee of our consistency result. Finally, we apply our methodology to extreme quantile prediction for U.S. wage data (Angrist et al., 2009). The ERF algorithm is available as an R package on <https://github.com/nicolagnecco/erf>.

## 2 Background

### 2.1 Extreme Value Theory

The first challenge of extreme quantile regression is that only a few or even no data points exceed the quantiles of interest. This section considers the classical case of unconditional extremes without predictors. Let  $Y_1, \dots, Y_n$  be  $n$  independent copies of a real-valued random variable  $Y$ . The notion of an extreme quantile  $\tau = \tau_n$  is typically expressed relative to the sample size  $n$ . The expected

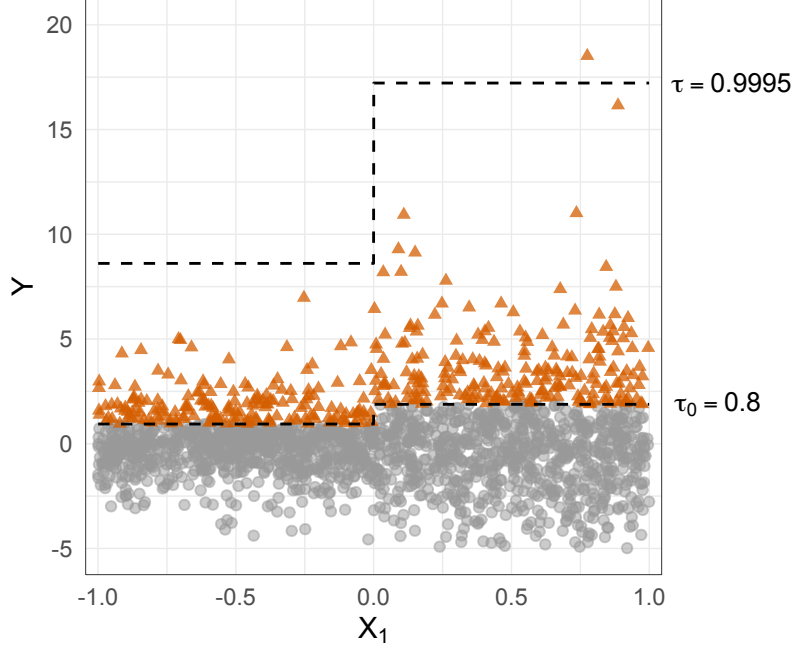


Figure 1: Realization of  $n = 2000$  samples from the generative model in Example 1 in Section 3.1. Response  $Y$  is plotted against the first predictor  $X_1$ . Dashed lines represent the quantile functions associated to the intermediate  $\tau_0 = 0.8$  and high  $\tau = 1 - 1/n = 0.9995$  quantile levels. Triangles are observations above the intermediate threshold.

number of observations in the sample that exceed the  $\tau_n$ -quantile is then  $n(1 - \tau_n)$ . A quantile with level  $\tau_n \rightarrow 1$  such that  $n(1 - \tau_n) \rightarrow \infty$  is called an intermediate quantile. Empirical estimation in this case still works well since the effective sample size, that is, the number of exceedances, grows to infinity (de Haan and Ferreira, 2006). For risk assessment, the most critical case is if the quantile of interest is eventually beyond the range of the data, that is,  $(1 - \tau_n)n \rightarrow 0$  as  $n \rightarrow \infty$ . Then, we can no longer rely on empirical estimators but must resort to asymptotically motivated approximations from extreme value theory.

Let  $u^* \in (0, \infty]$  be the upper endpoint of the distribution of  $Y$ . Under mild regularity assumptions on the tail of  $Y$ , the Pickands–Balkema–De Haan theorem (Balkema and de Haan, 1974; Pickands, 1975) states that there exists a normalizing function  $\sigma(u) > 0$  such that

$$\lim_{u \rightarrow u^*} \mathbb{P} \left( \frac{Y - u}{\sigma(u)} \leq z \mid Y > u \right) = G(z; (1, \xi)), \quad (2.1)$$

where the limit on the right-hand side is the distribution function of the generalized Pareto distribution (GPD) (Pickands, 1975) given by

$$G(z; \theta) = 1 - \left( 1 + \frac{\xi}{\sigma} z \right)_+^{-1/\xi}, \quad z > 0, \quad (2.2)$$

and  $\theta = (\sigma, \xi) \in (0, \infty) \times \mathbb{R}$  is the parameter vector consisting of scale and shape, respectively. The shape parameter  $\xi \in \mathbb{R}$ , also known as the extreme value index (Beirlant et al., 2005), characterizes

the decay of the tail of  $Y$ . If  $\xi > 0$ , then  $Y$  is heavy-tailed; if  $\xi = 0$ , then  $Y$  is light-tailed; if  $\xi < 0$  then  $Y$  has a finite upper endpoint. Moreover, the GPD is a natural model for the distribution tails since it is the only possible limit of threshold exceedances as in (2.1).

The GPD approximation can be directly translated into an approximation for the small probability of  $Y$  exceeding a high threshold  $y$ . By Bayes' theorem and (2.1) we obtain

$$\mathbb{P}(Y > y) = \mathbb{P}(Y > u) \mathbb{P}(Y > y \mid Y > u) \approx \mathbb{P}(Y > u) \{1 - G(y - u; \sigma, \xi)\},$$

where  $u < y$  denotes an intermediate threshold. Combining this approximation with (2.2) and letting  $\mathbb{P}(Y > y) = 1 - \tau$  and  $\mathbb{P}(Y > u) = 1 - \tau_0$ , we obtain an approximation for the  $\tau$ -quantile of  $Y$  as

$$Q(\tau) \approx Q(\tau_0) + \frac{\sigma}{\xi} \left[ \left( \frac{1 - \tau}{1 - \tau_0} \right)^{-\xi} - 1 \right], \quad (2.3)$$

where  $Q(\tau_0) := F_Y^{-1}(\tau_0)$  denotes the intermediate quantile at level  $\tau_0 < \tau$ .

In applications, the scale and shape parameters of the GPD have to be estimated from independent observations  $Y_1, \dots, Y_n$  of  $Y$ . We fix an intermediate quantile level  $\tau_0$  and define the exceedances  $Z_i = (Y_i - \hat{Q}(\tau_0))_+, i = 1, \dots, n$ , where  $\hat{Q}(\tau_0)$  denotes the empirical  $\tau_0$  quantile. We can estimate the GPD parameter vector  $\theta$  by maximum-likelihood, where the negative log-likelihood (or deviance) contribution of the  $i$ th exceedance  $Z_i$  is

$$\ell_\theta(Z_i) = \log \sigma + \left(1 + \frac{1}{\xi}\right) \log \left(1 + \frac{\xi}{\sigma} Z_i\right), \quad \theta \in (0, \infty) \times \mathbb{R}, \quad (2.4)$$

if  $Z_i > 0$ , and zero otherwise.

## 2.2 Quantile Regression and Generalized Random Forests

Given a pair  $(X, Y)$  of predictor vector  $X \in \mathbb{R}^p$  and response variable  $Y \in \mathbb{R}$ , quantile regression deals with modeling the conditional  $\tau$ -quantile  $Q_x(\tau)$  of the conditional distribution of  $Y$  given that  $X = x$  for a particular predictor value  $x \in \mathbb{R}^p$ . The main challenge is that the dimension  $p$  of the predictor space may be large and that the quantile surface  $Q_x(\tau)$  as a function  $x$  may be a complex, highly non-linear function.

Let  $(X_1, Y_1), \dots, (X_n, Y_n)$  be  $n$  independent copies of the random vector  $(X, Y)$ . In contrast to the setting in Section 2.1, classical methods for quantile regression consider a fixed quantile level  $\tau \equiv \tau_n$  that does not change with the sample size. On population level, these methods exploit the fact that the conditional quantile function is the minimizer of the expectation of the quantile loss  $\rho_\tau(c) = c(\tau - \mathbb{1}\{c < 0\})$ ,  $c \in \mathbb{R}$ , (Koenker and Bassett, 1978), that is,

$$Q_x(\tau) = \arg \min_{q \in \mathbb{R}} \mathbb{E}[\rho_\tau(Y - q) \mid X = x]. \quad (2.5)$$

The above expectation cannot be estimated directly on the sample level since the set of observed predictor values does not typically include the value  $x$ . A natural estimator is

$$\hat{Q}_x(\tau) = \arg \min_{q \in \mathbb{R}} \sum_{i=1}^n w_n(x, X_i) \rho_\tau(Y_i - q), \quad (2.6)$$

where  $x' \mapsto w_n(x, x')$  is a set of localizing similarity weights around the predictor value of interest. The weights can for instance be obtained by a kernel approach (Yu and Jones, 1998), but this is limited to moderately large dimensions (Stone, 1980, 1982).

In order to model more complex quantile surfaces in larger dimensions, Meinshausen (2006) and Athey et al. (2019) propose to use the estimator (2.6) with similarity weights  $w_n(\cdot, \cdot)$  obtained from a random forest. Random forests (Breiman, 2001) are an ensemble method used for both regression and classification tasks and consist of fitting  $B$  decision trees to the training data. In regression settings, each decision tree predicts a test point  $x \in \mathbb{R}^p$  by

$$\mu_b(x) := \sum_{i=1}^n \frac{\mathbb{1}\{X_i \in L_b(x)\} Y_i}{|\{i : X_i \in L_b(x)\}|}, \quad b = 1, \dots, B,$$

where  $L_b(x) \subset \mathbb{R}^p$  denotes the rectangular region that  $x$  belongs to in  $b$ th tree. By defining the similarity weights  $w_{n,b}(x, X_i) := \mathbb{1}\{X_i \in L_b(x)\} / |\{i : X_i \in L_b(x)\}|$ , the random forest predictions can be written as

$$\mu(x) := \frac{1}{B} \sum_{b=1}^B \mu_b(x) = \sum_{i=1}^n w_n(x, X_i) Y_i,$$

where  $w_{n,b}(x, X_i) = \sum_{b=1}^B w_{n,b}(x, X_i) / B$  is the average weight across  $B$  trees.

The original idea of Meinshausen (2006) is to use the weights estimated by this standard regression random forest for quantile regression in (2.6). A drawback of this approach is that the similarity weights arise from decision trees that are grown by minimizing the mean squared error loss. This leads to the fact that, as stated in Meinshausen (2006),  $w_n(x, X_i)$  takes large values for those observations  $i$  such that  $\mathbb{E}[Y | X = X_i] \approx \mathbb{E}[Y | X = x]$ . In many situations the conditional expectation is not representative of the whole conditional distribution of  $Y | X = x$ , and it may happen that  $w_n(x, X_i)$  is large but  $Q_{X_i}(\tau) \neq Q_x(\tau)$ ; see Athey et al. (2019, Figure 2) or our Figure 1 where the conditional expectation is constant over the predictor space. In these cases, the similarity weights estimated with standard random forest do not capture the heterogeneity of the quantile function and are thus not well-suited for quantile regression tasks. Athey et al. (2019) introduced generalized random forests (GRF), a method designed to fit random forests with custom loss functions. The GRF retains all the appealing features of classical random forests, i.e., it is simple to fit and requires little tuning of hyperparameters. One of the main applications of GRF is quantile regression, where the trees of the forest are grown to minimize the quantile loss function. In this work, we rely on GRF with quantile loss to estimate similarity weights  $w_n(\cdot, \cdot)$  that capture the variation of the entire conditional distribution of  $Y | X = x$  in the predictor space. In practice, the GRF algorithm estimates simultaneously conditional quantiles at levels  $\tau = 0.1, 0.5, 0.9$  as a proxy for the conditional distribution of  $Y | X = x$ . For simplicity, in the sequel, we refer to GRF with quantile loss as GRF.



## 3 Extremal Random Forest

### 3.1 The Algorithm

In this work we study a method for flexible extreme quantile regression where both challenges described in Sections 2.1 and 2.2 occur simultaneously. Consider the random vector  $(X, Y)$  of predictors  $X \in \mathcal{X} \subset \mathbb{R}^p$  and response  $Y \in \mathbb{R}$ , with  $\mathcal{X}$  compact. Let  $(X_1, Y_1), \dots, (X_n, Y_n)$  be independent copies of  $(X, Y)$ . In many applications in risk assessment, the goal is to estimate the quantile function  $x \mapsto Q_x(\tau) = F_{Y|X=x}^{-1}(\tau)$ , at an extreme level  $\tau = \tau_n$ , where the expected number of observations in the sample that exceed their conditional quantiles is small and possibly tends to 0 as  $n \rightarrow \infty$ ; see Section 2.1. To illustrate the challenges of this estimation problem, we consider an example where the scale of the response variable  $Y$  is modeled as a step function of the covariates  $X$ . This corresponds to [Athey et al. \(2019, Figure 2\)](#), except that we assume that the noise of the response variable is heavy-tailed instead of Gaussian.

*Example 1.* Let  $X \sim U_p$  be a uniform distribution on the cube  $[-1, 1]^p$  in dimension  $p$  and  $Y | X = x \sim s(x) T_\nu$ , where  $T_\nu$  denotes a Student's  $t$ -distribution with  $\nu > 0$  degrees of freedom. The shape parameter of the conditional distribution  $Y | X = x$  is then constant  $\xi(x) = 1/\nu(x) \equiv 0.25$  and we choose the  $s(x) = 1 + \mathbb{1}\{x_1 > 0\}$  for  $x \in \mathbb{R}^p$ . The GPD scale parameter  $\sigma(x)$  of  $Y | X = x$  and therefore also the quantile function  $Q_x(\tau)$  only depend on  $X_1$ . The other predictors are noise variables.

Figure 1 in the introduction shows  $n = 2000$  observations sampled from the model of Example 1 in dimension  $p = 40$ . The goal is to predict the conditional quantile  $Q_x(\tau)$  for a high level of  $\tau$ , e.g.,  $\tau = 0.9995$ . We observe that the difficulty of the task is twofold. First, because of a possibly high-dimensional predictor space, there might be no training observations close to  $x$ ; note that we only show the first of the 40 dimensions of  $X$  in the figure. Second, the  $\tau$ -quantile might be out of the range of the data if  $\tau$  is very close to one. Indeed, for a sample of size  $n$ , the expected number of exceedances above the conditional  $\tau$ -quantile is  $n(1 - \tau)$ , which becomes smaller than one if  $\tau > 1 - 1/n$ .

Our methodology accurately addresses both of these challenges. For effective localizing in the predictor space, even in high-dimensional problems, we use the weights emerging from GRF ([Athey et al., 2019](#)). For correct extrapolation in the tail of the conditional response variable, we rely on the asymptotic theory of extremes and fit a localized generalized Pareto distribution; see Section 2.1. More precisely, for an intermediate quantile level  $\tau_0$ , we assume that the distribution function of  $Y - Q_x(\tau_0)$ , conditional on  $Y > Q_x(\tau_0)$ , is approximately generalized Pareto ([Balkema and de Haan, 1974](#)) with scale and shape parameters depending on the predictor value  $x$ , that is, for any  $z > 0$ ,

$$\mathbb{P}(Y - Q_x(\tau_0) \leq z | Y > Q_x(\tau_0), X = x) \approx G(z; \theta(x)), \quad (3.1)$$

where  $\theta(x) = (\sigma(x), \xi(x))$ , and the scale and shape are continuous functions  $\sigma : \mathcal{X} \rightarrow (0, \infty)$  and  $\xi : \mathcal{X} \rightarrow \mathbb{R}$ , respectively. This assumption is a conditional version of (2.1) and means that the GPD approximation holds for the distribution of  $Y | X = x$  for any  $x \in \mathcal{X}$ . It is satisfied by most data generating processes as for instance in Example 1.

In order to formulate our estimators of the conditional GPD parameters  $\theta(x)$  and the extreme quantile  $Q_x(\tau)$ , we define the exceedances in the training data as

$$Z_i := (Y_i - \hat{Q}_{X_i}(\tau_0))_+, \quad i = 1, \dots, n; \quad (3.2)$$

see the triangles in Figure 1. Here,  $\tau_0 \in (0, 1)$  is an intermediate probability level that is chosen such that the estimator  $\hat{Q}_x(\tau_0)$  of the conditional quantile function can be obtained by classical quantile regression techniques; see Section 2.2. In principle, any quantile regression method can be used to fit  $Q_x(\tau_0)$ . Here, we choose GRF with quantile loss (Athey et al., 2019) since it is a flexible method well-suited for high-dimensional quantile regression problems and it requires little tuning.

For the estimation of the GPD parameter vector  $\theta(x) = (\sigma(x), \xi(x))$  we rely on those exceedances that carry most information on the tail of the distribution of  $Y | X = x$ . To do so, we use the localizing weight functions  $w_n(x, X_i)$  estimated from a GRF (Athey et al., 2019) that may be *different* from the one used to estimate the intermediate quantile  $\hat{Q}_x(\tau_0)$ . We would like to define the estimator of the conditional GPD parameter  $\hat{\theta}(x)$  as the minimizer of the weighted (negative) log-likelihood

$$L_n(\theta; x) = \sum_{i=1}^n w_n(x, X_i) \ell_\theta(Z_i) 1\{Z_i > 0\}, \quad x \in \mathcal{X}, \quad (3.3)$$

where  $\ell_\theta$  is defined in (2.4). In practice, the parameter space  $\theta(\mathcal{X}) = \{\vartheta \in (0, \infty) \times \mathbb{R} : \vartheta = \theta(x) \text{ for some } x \in \mathcal{X}\}$  is unknown. As explained by Dombry (2015), it is not guaranteed that the log-likelihood of the generalized extreme value distribution has a global optimum over the parameter space  $(0, \infty) \times \mathbb{R}$ . In fact, Smith (1985) shows that there exists no maximum likelihood estimator when  $\xi \leq -1$ . Analogous results apply to the GPD log-likelihood  $L_n(\theta; x)$  (Drees et al., 2004). We therefore follow Bücher and Segers (2017) and define  $\hat{\theta}(x)$  as the optimizer of  $L_n(\theta; x)$  over an arbitrarily large compact set  $\Theta \subset (0, \infty) \times (-1, \infty)$  such that  $\theta(\mathcal{X}) \subset \text{Int } \Theta$ , that is,

$$\hat{\theta}(x) = \arg \min_{\theta \in \Theta} L_n(\theta; x). \quad (3.4)$$

If there is more than one minimizer, let  $\hat{\theta}(x)$  be the smallest with respect to lexicographic order (see Dombry, 2015). The estimated pair  $(\hat{Q}_x(\tau_0), \hat{\theta}(x))$  of intermediate quantile and conditional GPD parameters can be plugged into the extrapolation formula (1.1) to obtain an estimate  $\hat{Q}_x(\tau)$  of the extreme conditional quantile at level  $\tau > \tau_0$ .

In Algorithm 1, we describe our prediction method, which we call the extremal random forest (ERF). The algorithm consists of two subroutines, namely ERF-FIT and ERF-PREDICT. The first one estimates a similarity weight function  $(x, y) \mapsto w_n(x, y)$  and an intermediate quantile function  $x \mapsto \hat{Q}_x(\tau_0)$  from the training data, for  $x, y \in \mathcal{X}$ . The second procedure predicts the extreme  $\tau$ -quantile  $\hat{Q}_x(\tau)$  at point  $x \in \mathcal{X}$  by estimating the GPD parameter vector  $\theta(x)$  as in (3.4). Appendix C shows the estimated GRF weights  $w_n(x, X_i)$  used in the likelihood in (3.3) for Example 1 and specific values of  $x$ . It can be seen that the weights are large for training observations  $X_i$  where the distribution of  $Y | X = X_i$  is equal to the one of  $Y | X = x$ .



---

**Algorithm 1** Extremal random forest (ERF)

---

Denote by  $\mathcal{D} = \{(X_i, Y_i)\}_{i=1}^n$  the training data. Let  $x \in \mathbb{R}^p$  be a test predictor value. Specify intermediate and extreme quantile levels  $\tau_0$  and  $\tau$ , respectively, with  $\tau_0 < \tau$ . Let  $\alpha$  be a vector of hyperparameters supplied to GRF.

- 1: **procedure** ERF-FIT( $\mathcal{D}, \tau_0, \alpha$ )
- 2:    $w_n(\cdot, \cdot) \leftarrow \text{GRF}(\mathcal{D}, \alpha)$
- 3:    $\hat{Q}(\cdot)(\tau_0) \leftarrow \text{QUANTILEREGRESSION}(\mathcal{D})$
- 4:   **output** erf  $\leftarrow [\mathcal{D}, w_n(\cdot, \cdot), \hat{Q}(\cdot)(\tau_0)]$
- 1: **procedure** ERF-PREDICT(erf,  $x, \tau$ )
- 2:    $Z_i \leftarrow (Y_i - \hat{Q}_{X_i}(\tau_0))_+$ , with  $i = 1, \dots, n$
- 3:    $\hat{\theta}(x) \leftarrow \arg \min_{\theta} L_n(\theta; x)$  as in (3.3)
- 4:   **output**  $\hat{Q}_x(\tau)$  as in (1.1)

The subroutine GRF estimates the similarity weight function  $w_n(\cdot, \cdot)$  using the generalized random forest of [Athey et al. \(2019\)](#). The subroutine QUANTILEREGRESSION fits the intermediate conditional quantile function  $\hat{Q}(\cdot)(\tau_0)$  using a classical quantile regression technique. The object erf is a list containing the training data  $\mathcal{D}$ , the fitted intermediate quantile  $\hat{Q}(\cdot)(\tau_0)$ , and the estimated similarity weight function  $w_n(\cdot, \cdot)$ .

---

## 3.2 Consistency

Our ERF provides an estimate  $\hat{\theta}(x) = (\hat{\sigma}(x), \hat{\xi}(x))$  of the conditional GPD parameter  $\theta(x)$  that describes the tail of the distribution of  $Y \mid X = x$ . The method is at the interface of random forests and extreme value theory, and both fields have their challenges related to the analysis of asymptotic properties.

Consistency and asymptotic normality of classical ([Meinshausen, 2006](#); [Biau, 2012](#); [Scornet et al., 2015](#); [Wager and Athey, 2018](#)) and generalized random forests ([Athey et al., 2019](#)) have only recently been established. The results by [Athey et al. \(2019\)](#) require regularity conditions (see Assumptions 1–6 of their paper) that are not satisfied in our setting. In particular, the negative GPD log-likelihood  $\theta \mapsto \ell_{\theta}(z)$  that we consider is not a convex function and, therefore, it does not satisfy Assumption 6 in [Athey et al. \(2019\)](#). On the other hand, the asymptotic analysis of extreme value estimators is notoriously difficult due to the pre-limit approximation in (3.1) and changing distributional support ([Smith, 1985](#); [Drees et al., 2004](#)). Recent papers have worked out the asymptotics for the unconditional i.i.d. case ([Dombry, 2015](#); [Bücher and Segers, 2017](#); [Dombry and Ferreira, 2019](#)).

We will not show consistency of the ERF under the most general conditions on the distributional tail of  $Y \mid X = x$  since the required technicalities would be beyond the scope of this paper. We list all assumptions needed for our theorem and discuss possible relaxations after the statement. The first assumption deals with the data generating process.

**Assumption 1.** Let  $X \in \mathcal{X}$  have a density that is bounded away from 0 and  $\infty$  and support  $\mathcal{X} := [0, 1]^p$ . For large enough  $\tau_0$ , suppose the conditional intermediate quantile function  $Q_X(\tau_0)$  is known. Furthermore, assume that the distribution function of  $Y - Q_X(\tau_0)$ , conditional on

$Y > Q_X(\tau_0)$ , is *exactly* generalized Pareto with parameter vector  $\theta(X)$ .

The next assumption addresses how the parameter vector  $\theta(x)$  depends on the predictor  $X = x$ . We consider only the most relevant case of positive shape parameter  $\xi(x) > 0$ , that is, where  $Y \mid X = x$  is heavy-tailed.

**Assumption 2.** Let  $\theta(x) = (\sigma(x), \xi(x))$  denote the bivariate regression function for the GPD parameters, for  $x \in \mathcal{X}$ . Assume  $\sigma : \mathcal{X} \rightarrow (0, \infty)$  and  $\xi : \mathcal{X} \rightarrow (0, \infty)$  are continuous functions on  $\mathcal{X}$ . Furthermore, assume their first order partial derivatives are continuous in the interior and exist on the boundary of  $\mathcal{X}$ ; we refer to Appendix B for a definition of partial derivative on the boundary. Notice that the parameter space  $\theta(\mathcal{X}) \subset (0, \infty) \times (0, \infty)$  is compact and bounded away from the origin.

Let  $(X_1, Y_1), \dots, (X_n, Y_n)$  be independent copies of  $(X, Y)$ . The first step of our algorithm consists of fitting a generalized random forest on the training data to obtain similarity weights. To show consistency, we make the following standard assumptions on how this forest is built.

**Assumption 3.** Let  $w_n(x, y)$  denote the similarity weights for  $x, y \in \mathcal{X}$  estimated by a GRF. We assume the forest satisfies Specification 1 of [Athey et al. \(2019\)](#). In particular, we assume that each tree in the forest is symmetric, places balanced splits, and is randomized (see [Athey et al., 2019](#)). We require that each tree is fitted on a subsample of the training data with size  $s < n$ , such that  $s \rightarrow \infty$  and  $s/n \rightarrow 0$  as  $n \rightarrow \infty$ , and that the forest consists of  $\binom{n}{s}$  trees fitted on all possible subsamples of size  $s$ .

In practice, one builds a forest by estimating  $B$  trees. Our theoretical results hold for forests made of  $\binom{n}{s}$  trees fitted on all possible subsamples of size  $s$ . For this reason, similarly to [Wager and Athey \(2018\)](#), we assume that  $B$  is large enough so that the Monte Carlo effect is negligible. Furthermore, Assumption 3 does not require that the trees in the forest are honest in the sense of [Athey et al. \(2019\)](#). The reason is that, as opposed to [Athey et al. \(2019\)](#), our conditional response distribution belongs to the parametric GPD family. In practice, we find that honesty helps our algorithm perform better, and the result below remains true under this additional, stronger assumption.

**Theorem 1.** *Let  $(X_1, Y_1), \dots, (X_n, Y_n)$  be independent copies of  $(X, Y)$  as specified in Assumptions 1 and 2. Let  $x \in \text{Int } \mathcal{X}$  be a fixed test predictor value, and denote by  $w_n(x, X_i)$  the similarity weights estimated with a forest satisfying Assumption 3. Let  $\Theta \subset (0, \infty) \times (0, \infty)$  be an arbitrary compact set such that  $\theta(\mathcal{X}) \subset \text{Int}(\Theta)$ , and let  $\hat{\theta}(x)$  denote a sequence of estimators minimizing (3.3). Then,  $\hat{\theta}(x) \rightarrow \theta(x)$  in probability as  $n \rightarrow \infty$ .*

The proof relies on the theory of [Newey \(1991\)](#) and is in Appendix A. To the best of our knowledge, this is the first consistency proof for a tree-based extreme quantile regression method that works for high-dimensional predictor spaces and complex parameter response surfaces. [Wang and Tsai \(2009\)](#) show asymptotic normality for the model parameters for the heavy-tailed case, but only in the situation where the covariate dependence is linear. There are no asymptotic results for models for generalized Pareto distributions with parameters depending in a more complex way on

the covariates such as through generalized additive models (Chavez-Demoulin and Davison, 2005; Youngman, 2019), trees (Farkas et al., 2020) or gradient boosting (Velthoen et al., 2021).

Similarly to Wang and Tsai (2009), we focus on the heavy-tailed case where  $\xi(x) > 0$  for all  $x \in \mathcal{X}$ . Relaxing this assumption to  $\xi(x) \in \mathbb{R}$  would make the support of the generalized Pareto distribution depend on the model parameters. This would require a different proof strategy and additional care in terms of Lipschitz conditions, but some ideas from the i.i.d. case in Bücher and Segers (2017, Lemma E.2) might be helpful.

A further simplification in our setup is that we assume that the approximation in (3.1) is an equality. Dropping this assumption would require additional conditions to control the approximation error and would add a further level of technicality to the proofs. Similar assumptions are often made in the literature as for instance in Bücher and Segers (2017) for the i.i.d. case for generalized extreme value distributions.

### 3.3 Hyperparameter Tuning

Generalized random forests have several tuning parameters, such as the number of predictors selected at each split and the minimum node size. This section presents a cross-validation scheme to tune such hyperparameters within our algorithm. For large values of  $\tau \approx 1$ , the quantile loss is not a reliable scoring function since there might be few or no test observations above this level. In our case, we can instead rely on the tail approximation in (3.1) and use the deviance of the GPD as a reasonable metric for cross-validation. Let  $\mathcal{N}_1, \dots, \mathcal{N}_M$  be a random partitioning of  $\{1, \dots, n\}$  into  $M$  equally sized folds of the training data. For a sequence  $\alpha_1, \dots, \alpha_J$  of tuning parameters, we fit an `erf` object on the training set  $(X_i, Y_i)$ ,  $i \notin \mathcal{N}_m$ , for each  $\alpha_j$  and each fold  $m$  as described in the `ERF-FIT` function in Algorithm 1. Given the fitted `erf` object, we estimate the GPD parameter vector  $\hat{\theta}(X_i; \alpha_j)$  on the validation set  $(X_i, Y_i)$ ,  $i \in \mathcal{N}_m$  as in the `ERF-PREDICT` function in Algorithm 1, and evaluate the cross-validation error by

$$CV(\alpha_j) = \sum_{m=1}^M \sum_{i \in \mathcal{N}_m} \ell_{\hat{\theta}(X_i; \alpha_j)}(Z_i) 1\{Z_i > 0\},$$

where  $\theta \mapsto \ell_\theta(z)$  is the deviance of the GPD and  $Z_i := (Y_i - \hat{Q}_{X_i}(\tau_0))_+$  are the exceedances. Finally, we select the optimal tuning parameter  $\alpha^*$  as the minimizer of  $CV(\alpha_j)$ ,  $j = 1, \dots, J$ . To make the problem computationally tractable, we first fit the intermediate quantile function  $x \mapsto \hat{Q}_x(\tau_0)$  on the entire data set. Then, on each fold, we estimate the similarity weight function  $(x, y) \mapsto w_n(x, y)$  with “small” forests made of 50 trees. We repeat the cross-validation scheme several times to reduce the variability of the results.

Even though, in principle, one could perform cross-validation on several tuning parameters, we find that the minimum node size  $\kappa \in \mathbb{N}$  plays the most critical role for ERF. The reason is that  $\kappa$  controls the model complexity of the individual trees in the forest and consequently of the similarity weights  $w_n(\cdot, \cdot)$ . Small (large) values of  $\kappa$  correspond to trees with few (many) observations in each leaf and produce strongly (weakly) localized weight functions  $w_n(\cdot, \cdot)$ . The estimates of the shape parameter  $\hat{\xi}(x)$  in (3.4) may be sensitive to small changes of the localizing weights in the covariate space, leading to unstable quantile predictions through (1.1). To reduce the variance of

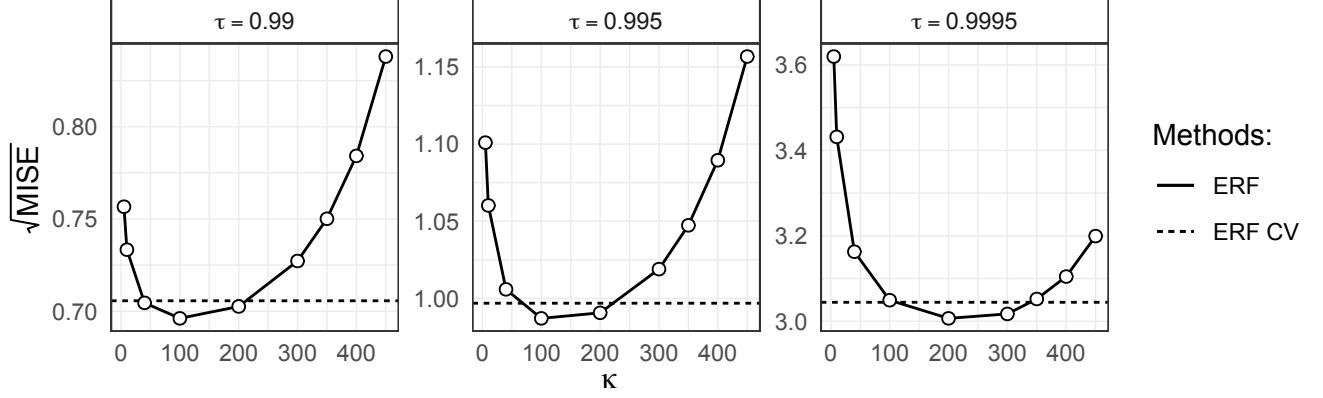


Figure 2: Solid line shows the square root of the MISE of ERF for different minimum node sizes  $\kappa$  over 50 simulations. The dashed line shows the square root MISE of the cross-validated ERF. The data is generated according to Example 1.

$\hat{\xi}(x)$ , it is useful to stabilize the log-likelihood  $x \mapsto L_n(\theta; x)$  by estimating the similarity weights  $w_n(\cdot, \cdot)$  with a forest made of trees with relatively large leaves. Notice that  $w_n(x, y)$  influences the effective number of observations used in the weighted (negative) log-likelihood  $L_n(\theta; x)$  (3.3).

Figure 2 shows numerical results of cross-validating the minimum node size  $\kappa$  for the model described in Example 1. Here, we perform 5-fold cross-validation repeated three times by growing forests of 50 trees on each fold. We measure the performance as the square root of the mean integrated squared error (MISE) between the estimated and the true quantile function over 50 simulations; see Section 4 for the definition of the MISE. We observe that the cross-validated performance of ERF (dashed line) is close to the minimum square root MISE, suggesting that the proposed cross-validation scheme works well.

### 3.4 Penalized Log-Likelihood

The shape  $\xi$  of the GPD is the most crucial parameter since it determines the tail behavior of  $Y$  at extreme quantile levels; the extrapolation formula (2.3) shows the highly non-linear influence of the shape parameter on large quantiles.

Estimation of the shape parameter is notoriously challenging, and the maximization of the GPD likelihood may exhibit convergence problems for small sample sizes (Coles and Dixon, 1999). In general, penalization can help to reduce the variance of an estimator at the cost of higher bias (Hastie et al., 2009). Coles and Dixon (1999) propose a penalty function that restricts the shape parameter values to  $\xi < 1$  and favors smaller values of  $\xi$ . Several penalization schemes can be interpreted in a Bayesian sense by considering a prior distribution on the regularized parameter. For example, de Zea Bermudez and Turkman (2003) introduce a Bayesian approach to estimate the  $\xi$  by using different priors for the cases  $\xi > 0$  and  $\xi < 0$ , respectively. In the context of the generalized extreme value distribution, other penalization methods have been proposed by Smith and Naylor (1987).

While the above regularization methods are tailored to i.i.d. data, in our setting we want to

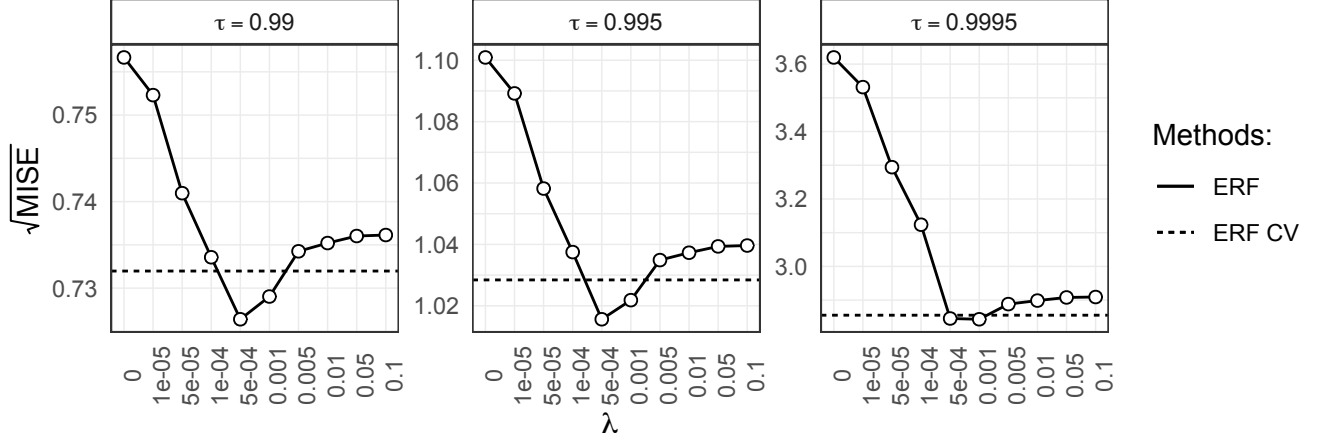


Figure 3: Square root MISE of ERF for different penalty values  $\lambda$  and quantile levels  $\tau$  over 50 simulations. The data is generated according to Example 1.

penalize the variation of the shape function  $x \mapsto \xi(x)$  across the predictor space  $\mathcal{X}$ . In spatial applications, for instance, it is common to assume a constant shape parameter at different locations (e.g., Ferreira et al., 2012; Engelke et al., 2019). Similarly, in ERF we shrink the estimates  $\hat{\xi}(x)$  to a constant shape parameter  $\xi_0$ . In general,  $\xi_0$  can be given by expert knowledge, but often a good choice is the unconditional fit  $\xi_0 = \hat{\xi}$  obtained by minimizing the GPD deviance in (3.3) with constant weights  $w_n(x, y) = 1$  for all  $x, y \in \mathcal{X}$ .

We propose to penalize the weighted GPD deviance (3.3) with the squared distance between the estimates of  $\xi(x)$  and the constant shape parameter  $\xi_0$ , that is,

$$\hat{\theta}(x) = \arg \min_{(\sigma, \xi) = \theta \in \Theta} \frac{1}{(1 - \tau_0)} L_n(\theta; x) + \lambda(\xi - \xi_0)^2, \quad (3.5)$$

where  $\lambda \geq 0$  is a tuning parameter, and  $\tau_0$  is the intermediate quantile level. The parameter  $\lambda$  allows interpolating between a simpler model with a constant shape when  $\lambda \rightarrow \infty$ , and a more complex model with a varying shape over the predictor space when  $\lambda$  is small. This penalized negative log-likelihood can be interpreted in a Bayesian sense: it is equivalent to the maximum *a posteriori* GPD estimator when putting Gaussian prior  $N(\xi_0, 1/(2\lambda))$  on the shape parameter  $\xi$ . Bücher et al. (2020) propose the same penalization as in (3.5) to estimate the generalized extreme value distribution parameters, where the prior distribution is centered around an expert belief  $\xi_0$  and  $\lambda \geq 0$  reflects the confidence in such belief.

In practice, when we penalize the shape parameter we modify Algorithm 1 by replacing Line 3 of the ERF-PREDICT subroutine with (3.5). Similarly, we cross-validate  $\lambda$  using the scheme presented in Section 3.3 on the modified Algorithm 1. Figure 3 shows the square root MISE over 50 simulations for different values of  $\lambda$  and different quantile levels. Here, we set  $\xi_0$  as the estimated unconditional shape parameter.

## 4 Simulation Study

### 4.1 Setup

We compare ERF to other quantile regression methods on simulated data sets, assessing the properties of the different approaches. In the three experiments, we simulate  $n$  training observations  $(X_1, Y_1), \dots, (X_n, Y_n)$  as independent copies of a random vector  $(X, Y)$ . We always generate the predictor  $X \in \mathbb{R}^p$  from a uniform distribution on the cube  $[-1, 1]^p$  for different dimensions  $p$ . We let the conditional response variable  $Y \mid X = x$  follow distributions such as Gaussian or Student's  $t$ , with tail heaviness depending on the simulation study. The parameters of these distributions, and therefore also the parameters of the GPD corresponding to their tails, vary as functions of the predictor value  $x$ . Different response surfaces are considered. The goal is to predict the quantiles  $Q_x(\tau)$  of the conditional response  $Y \mid X = x$  for moderately to very extreme quantile levels  $\tau > 0$ .

We evaluate the performance of the method on a test data set  $\{x_i\}_{i=1}^{n'}$  of  $n' = 1000$  observations generated with a Halton sequence (Halton, 1964) on the cube  $[-1, 1]^p$ . For a fitted quantile regression function  $x \mapsto \hat{Q}_x(\tau)$ ,  $\tau \in (0, 1)$ , we then compute the integrated squared error (ISE) on the test data set as

$$\text{ISE} = \frac{1}{n'} \sum_{i=1}^{n'} \left( \hat{Q}_{x_i}(\tau) - Q_{x_i}(\tau) \right)^2,$$

where  $x \mapsto Q_x(\tau)$  is the true quantile function of the model. Repeating the simulation, fitting and evaluation  $m = 50$  times, we obtain the mean integrated squared error (MISE) as the average of the different ISEs.

In the first experiment, we study how ERF performs on the two challenges of high quantile levels and high-dimensional predictor spaces illustrated in Figure 1. The data sets follow the model of Example 1 where the response has a Student's  $t$ -distribution with scale shift according to a step function. We consider the methods' performances for different dimensions  $p$  of the predictor space and different quantile levels  $\tau$ .

The second experiment studies the robustness of ERF and other methods to the tail heaviness of the noise distribution. The data generating function is the same as in the first experiment, except that the tail of the noise ranges from the light-tailed Gaussian case with  $\xi = 0$  to the relatively heavy tails of Student's  $t$  distributions with large  $\xi > 0$ .

In the last experiment (see Appendix D.2), we consider more complex regression functions for the conditional response variables to assess the performance of the quantile regression methods on complex data. The underlying models depend on more than one predictor value, and both the scale and the shape parameters vary simultaneously.

### 4.2 Competing Methods

Among the forest-based algorithms, we consider the quantile regression forest by Meinshausen (2006), denoted by QRF, and the generalized random forest by Athey et al. (2019), denoted by GRF. Since these methods do not rely on the GPD likelihood, it is not possible to cross-validate their tuning parameters as in Section 3.3 for prediction error of extreme quantiles. However, in



independent simulations, we notice that their tuning parameters do not have big influence on the results. We set their tuning parameters to the default values and fit the quantile functions  $\hat{Q}_x^{QRF}(\tau)$ ,  $\hat{Q}_x^{GRF}(\tau)$  on the training data for some  $\tau \in (0, 1)$ . More details on forest-based approaches can be found in Section 2.2.

As a hybrid method that uses forest-based weights, we consider the method EGP Tail proposed by Taillardat et al. (2019) who assume that the entire conditional distribution  $Y | X = x$  follows a parametric family called extended generalized Pareto (EGP) distribution. They estimate the covariate dependent parameters of the EGP through a probability-weighted method of moments using the estimated quantiles  $\hat{Q}_x^{GRF}(\tau)$  of the GRF. We follow the authors' implementation and use the default parameter values.

Our ERF method is part of the class of extrapolation approaches that model the exceedances  $Z_i$  in (3.2) by conditional GPD distributions. Among the numerous methods that follow this strategy we present only those from Youngman (2019) and Velthoen et al. (2021) as they turn out to be most competitive. Other existing extrapolation based methods are not flexible enough in our setting (Wang and Tsai, 2009; Wang et al., 2012) or do not perform well with larger noise dimensions (Daouia et al., 2011; Gardes and Stupfler, 2019). For the sake of comparability, for all extrapolation methods we use the same exceedances  $Z_i = (Y_i - \hat{Q}_x^{GRF}(\tau_0))_+$ , which are computed from a GRF with intermediate quantile level  $\tau_0 = 0.8 \leq \tau$ . To assess the sensitivity of our method to the intermediate threshold  $\tau_0$ , we perform a simulation study for a data set generated according to Example 1; see Figure 10 in Appendix D.1. In this setup, the intermediate threshold does not strongly influence the results. In general, the optimal choice will depend on the properties of the data (see de Haan and Ferreira, 2006, Section 3.2) and numerous data-driven methods for choosing the threshold exist (e.g., Embrechts et al., 2012, Section 6.2.2).

The method from Youngman (2019) uses generalized additive models to estimate the parameters of a GPD distribution. Here, we model the scale and shape parameters as smooth additive functions of the covariates without interaction effects. In the sequel, we abbreviate this method by EGAM. Velthoen et al. (2021) propose the GBEX method to estimate the GPD parameters using gradient boosting (Friedman, 2001, 2002). In particular, they grow two sequences of gradient trees to model the conditional scale and shape parameter, respectively. To fit GBEX, we use 5-fold cross validation with a maximum number of trees per fold set to  $B_{\max} = 500$ . We set the depth of each gradient tree  $D = 2$ , and we set the learning rate for the scale parameter to  $\lambda^\sigma = 0.1$ . We set the other tuning parameters to their default values. We also consider the unconditional model as a baseline, where we fit constant GPD parameters  $(\sigma, \xi)$  to the conditional exceedances  $Z_i$ .

Concerning our ERF method, we fit the parameters as described in Algorithm 1 using the repeated cross-validation scheme described in Section 3.3. In particular we repeat three times 5-fold cross-validation to tune the minimum node size  $\kappa \in \{10, 40, 100\}$  and the penalty  $\lambda \in \{0, 0.01, 0.001\}$  for the shape parameter. We leave the other tuning parameters of the random forests at their default values; see the documentation for `quantile_forest` in Tibshirani et al. (2021). All simulation results can be reproduced following the description and code on <https://github.com/nicolagnecco/erf-numerical-results>.

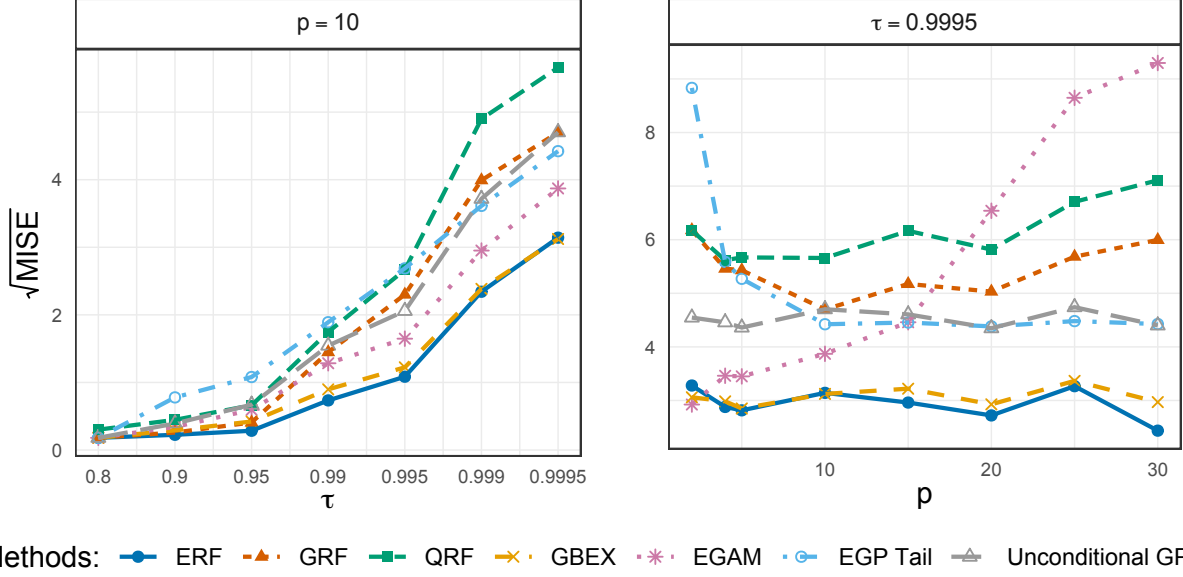


Figure 4: Square root MISE for different methods against the quantile level  $\tau$  in dimension  $p = 10$  (left), and against the model dimension  $p$  for quantile levels  $\tau = 0.9995$  (right).

### 4.3 Experiment 1

In this simulation study, the data follows the model of Example 1 where the response variable  $Y | X = x$  follows a Student's  $t$ -distribution with  $\nu(x) \equiv 1/\xi(x) = 4$  degrees of freedom and scale  $s(x) = 1 + \mathbb{1}\{x_1 > 0\}$ . This is the same setup as in the simulation in Athey et al. (2019, Section 5), except that here we use Student's  $t$ -distribution instead of Gaussian for the noise. There is only one signal variable  $X_1$  and  $p - 1$  noise variables. We generate  $n = 2000$  training data and consider different dimensions  $p$  and quantile levels  $\tau$ .

We first fix the dimension  $p = 10$  and investigate the effect of different target quantile levels  $\tau$  on the prediction performances of the competing methods. The left panel of Figure 4 shows the  $\sqrt{\text{MISE}}$ , the square root of the MISE defined in Section 4.1, for varying values of  $\tau$  close to 1. At the intermediate quantile level  $\tau_0 = 0.8$  all methods show a similar performance; in fact, the extrapolation methods coincide at this level since they use the same GRF based estimator for the intermediate quantile. When the quantile level  $\tau$  increases, or equivalently, the expected number of exceedances  $n(1 - \tau)$  in the training sample decreases, we observe that the performance curves diverge. The forest-based quantile regression methods that do not explicitly use extreme value theory for tail approximations cannot extrapolate well to extreme quantile levels. This includes the EGP Tail method that does not focus on modeling the tail. Among the extrapolation methods, the unconditional baseline does not perform well since it cannot capture the shift in the scale function. While the EGAM does better, it already suffers from the relatively high dimension of the noise variables, a fact that we discuss in detail below. By far, the best methods are our ERF and the GBEX. Both combine the flexibility in the predictor space with correct extrapolation originating from the GPD approximation.

We next compare the performances for varying dimensions  $p$  of the predictor space. The right

panel of Figure 4 shows the  $\sqrt{\text{MISE}}$  as a function of  $p$  for fixed quantile levels  $\tau = 0.9995$ . QRF and GRF look relatively robust against growing dimensions and additional noise variables, but the performance is not competitive for higher quantiles levels. For smaller dimensions, the methods deteriorate because of the overfitting; the trees can only place split on the signal variable  $X_1$ , increasing the variance. The performance of EGAM clearly illustrates the problem of this method with higher dimensions. The method cannot filter the signal from the many noise variables even though, in principle, it is flexible enough to model the response function; the latter is indicated by the good performance for very small noise dimension. Moreover, as mentioned by Youngman (2019), the method becomes computationally demanding as  $p$  grows. The unconditional model is unaffected by the noise dimension since it does not use the predictor values. Both ERF and GBEX combine the advantages of the two types of approaches. They are both robust against additional noise variables and perform well even for large dimensional predictor spaces.

## 4.4 Experiment 2

In the second experiment, we investigate the robustness of the quantile regression methods against noise distributions with different tail heaviness in a large dimension. The simulation setup is similar to the previous section and data follows the model of Example 1, where we set  $p = 40$ . We simulate data for noise distributions with shape parameters  $\xi = 0, 1/4, 1/3$ , where for the light-tailed case  $\xi = 0$  we choose a Gaussian distribution and otherwise a Student's  $t$  distribution with  $\xi = 1/4, 1/3$  corresponding  $\nu = 4, 3$  degrees of freedom, respectively. We exclude EGAM in this experiment since its performance decreases for large  $p$  and it becomes computationally prohibitive (see Figure 4).

Figure 5 shows boxplots of the  $\sqrt{\text{ISE}}$  for the extreme quantile level  $\tau = 0.9995$  for the different methods and different shape parameters. The triangles correspond to the average values. To make the plot easier to visualize, we remove large outliers of GRF and QRF. The picture is similar for the three noise distributions. We observe that ERF performs very well also in the Gaussian case. Since our method relies on the GPD, estimation is not restricted to positive shape parameters, as opposed to approaches based on the Hill estimator (e.g., Wang et al., 2012; Wang and Li, 2013). Unsurprisingly, as the noise becomes very heavy-tailed (right-hand side of Figure 5) the performances of all methods become closer since the problem becomes increasingly difficult. We further note that the performance of both QRF and GRF degrades for large values of  $\xi$ . They exhibit increasingly large outliers that result in an average exceeding the upper quartile. This underlines that classical methods without proper extrapolation are insufficient for extreme quantile regression.

## 5 Analysis of the U.S. Wage Structure

We compare the performance of ERF, GBEX, GRF, and the unconditional GPD on the U.S. census microdata for the year 1980 (Angrist et al., 2009). As described therein, the data set consists of 65,023 U.S.-born black and white men of age between 40–49, with five to twenty years of education, and with positive annual earnings and hours worked in the year before the census. The large number of observations makes this dataset suitable to assess the performance of the different

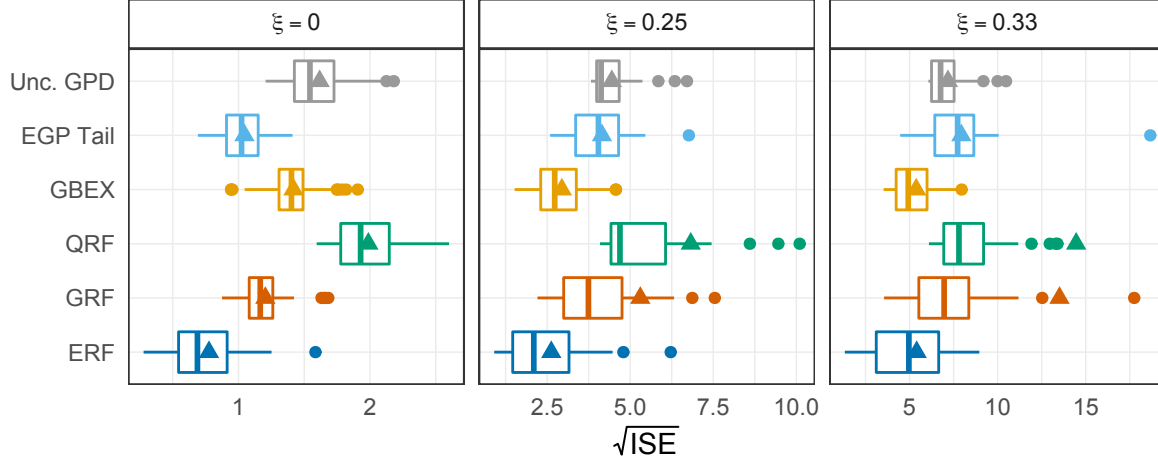


Figure 5: Boxplots of  $\sqrt{\text{ISE}}$  over  $m = 50$  simulations, for different tail indices in the noise distribution at the quantile level  $\tau = 0.9995$ . The predictor space dimension is  $p = 40$ . Triangles represent the average values.

methods at very high quantile levels. The response  $Y$  describes the weekly wage, expressed in 1989 U.S. dollars computed as the annual income divided by the number of weeks worked. The predictor vector consists of the numerical variables age and years of education and the categorical predictor whether the person is black or white. To make the data set higher dimensional, we add ten random predictors sampled independently from uniform distributions on the interval  $[-1, 1]$ , resulting in a predictor space's dimension  $p = 13$ .

Throughout this analysis, we fit ERF repeating three times 5-fold cross-validation to tune the minimum node size  $\kappa \in \{5, 40, 100\}$ . To stabilize the variance of the shape parameter, we set the penalty  $\lambda = 0.01$ . Regarding the other methods, we use the same tuning parameter setup as in 4.2. In particular, we use GRF to predict the intermediate conditional quantiles at level  $\tau_0 = 0.8$  for all extrapolation-based methods. We split the original data into two halves, i.e., 32,511 and 32,512 samples, respectively. We use the first portion to perform an exploratory data analysis and the second one to fit and evaluate the different methods.

For the exploratory data analysis, we fit ERF on a random subset made of 10% of the data (i.e., 3,251 observations), and predict the GPD parameters  $\hat{\theta}(x) = (\hat{\sigma}(x), \hat{\xi}(x))$  on the left-out observations (i.e., 29,260 observations). Figure 6 shows the estimated GPD parameters  $\hat{\theta}(x)$  as a function of years of education. We observe that the scale parameter depends positively on years of education, whereas it is quite homogeneous between the black and white groups. In particular, it has a clear jump around 15-16 years of education, which corresponds to the end of the undergraduate studies. The shape parameter is relatively homogeneous for the black and white group and looks stable for education. It ranges between 0.22 and 0.24, indicating heavy-tails throughout the predictor space. Moreover, Figure 12 in Appendix E.1 shows that the scale and shape parameters do not seem to depend on the predictor age.

In Figure 7 we compare the ERF quantile predictions to the ones obtained by the other methods at levels  $\tau = 0.9, 0.995$ . To help with the visualization, we removed all the quantiles above 6,000

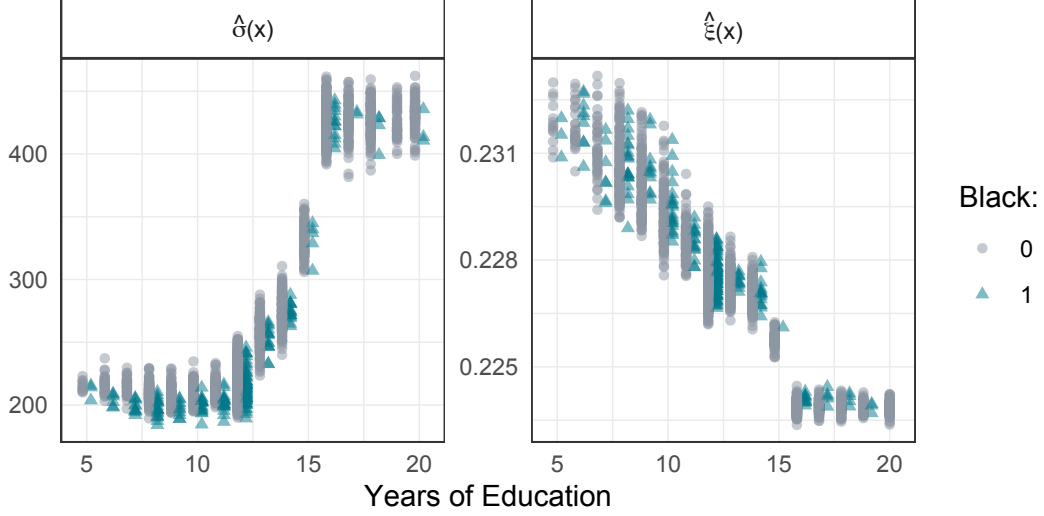


Figure 6: Estimated GPD parameters  $\hat{\theta}(x)$  as a function of the years of education for the black (triangles) and white (circles) subgroups.

predicted by GRF. We observe that the extrapolation methods retain a good shape of the quantile function even for high levels. This does not hold for GRF, whose profile worsens as  $\tau$  increases, and the discrete structure of the largest training observations becomes visible. The unconditional method seems to capture the variability of the conditional quantiles for  $\tau = 0.9$ , but we observe that it loses flexibility for larger values of  $\tau$ . The reason for this is that the unconditional method cannot produce different scale parameters of the GPD, while Figure 6 indicates that this is necessary for this data set. ERF and GBEX model well the variability of the conditional quantiles for all values of  $\tau$ , and they agree on the magnitude of the estimates.

After the exploratory analysis, we assess the quantitative performance of ERF compared to the other methods. We consider the prediction metric proposed by Wang and Li (2013),

$$\mathcal{R}_n(\hat{Q}(\tau)) := \frac{\sum_{i=1}^n \mathbb{1}\{Y_i < \hat{Q}_{X_i}(\tau)\} - n\tau}{\sqrt{n\tau(1-\tau)}}, \quad (5.1)$$

where  $n$  is the number of test observations, and  $\hat{Q}(\tau)$  is the  $\tau$ -th conditional quantile estimated on the training data set. This metric compares the normalized estimated proportion of observations with  $Y_i < \hat{Q}_{X_i}(\tau)$  with the theoretical level  $\tau$ . Using the true quantile function  $Q(\tau)$ , the random variable  $\mathbb{1}\{Y_i < Q_{X_i}(\tau)\}$  follows a Bernoulli distribution with expectation  $\tau$  and variance  $\tau(1-\tau)$ , and by the central limit theorem the metric with oracle quantile function  $\mathcal{R}_n(Q(\tau))$  is asymptotically standard normal. We partition the 32,512 observations not used in the exploratory analysis into ten random folds. On each fold, we fit the different methods and evaluate them on the left-out observations, using the absolute value of (5.1). Unlike classical cross-validation, we fit the methods using a single fold and validate them on the remaining ones; this allows us to have enough observations to gauge their performance for high quantile levels  $\tau$ . Figure 8 shows the performance of ERF, GRF, GBEX, and the unconditional method over the ten repetitions for different quantile levels. The shaded area represents the 95% interval of the absolute value of a standard normal distribution, corresponding

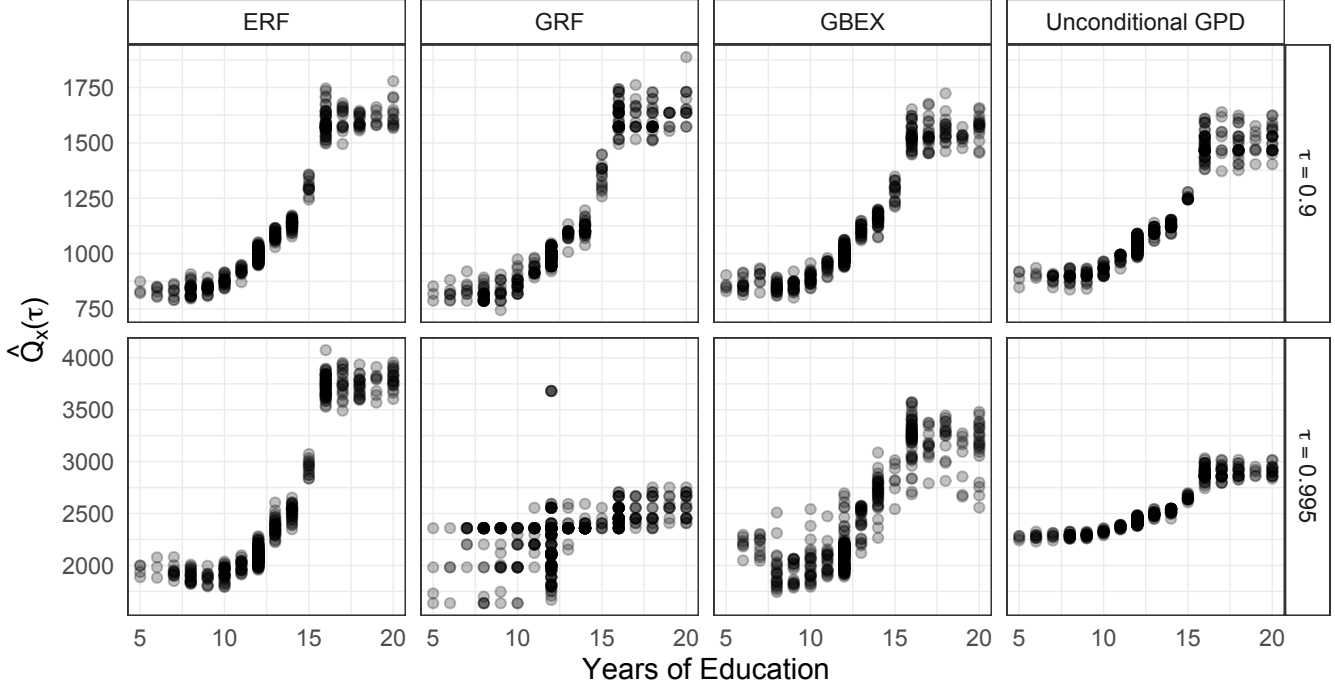


Figure 7: Predicted quantiles at levels  $\tau = 0.9, 0.995$  for ERF, GRF, GBEX, and the unconditional method.

to the 95% confidence level of the oracle method with true quantile function. We observe that both ERF and GBEX have very good performance compared to the oracle for increasing quantile levels, and they outperform the unconditional method for large values of  $\tau$ . This is because they are flexible to model the scale and shape as a function of the predictors, unlike the unconditional method. While GRF performs well for the quantile level  $\tau = 0.9$ , it worsens quite quickly for larger values of  $\tau$ . This is expected since GRF does not rely on extrapolation results from extreme value theory and cannot accurately predict very high quantiles.

For the same data set, [Angrist et al. \(2006\)](#) consider the natural logarithm of the wage as a response variable for quantile regression with fixed, non-extreme quantile levels. In [Appendix E.1](#) we perform our analysis above for extreme quantiles again with this log-transformed response since it highlights several interesting properties of the ERF algorithm. In particular, [Figure 14](#) in [Appendix E.2](#) shows that the flexible methods ERF and GBEX have the desirable property that the predictions do not change much under marginal transformations. The unconditional method, on the other hand, seems to be sensitive to marginal transformations; for an explanation and details, see [Appendix E.1](#). In general, therefore, it is advised to use a flexible extrapolation method, such as ERF or GBEX, that performs well on any marginal distributions.



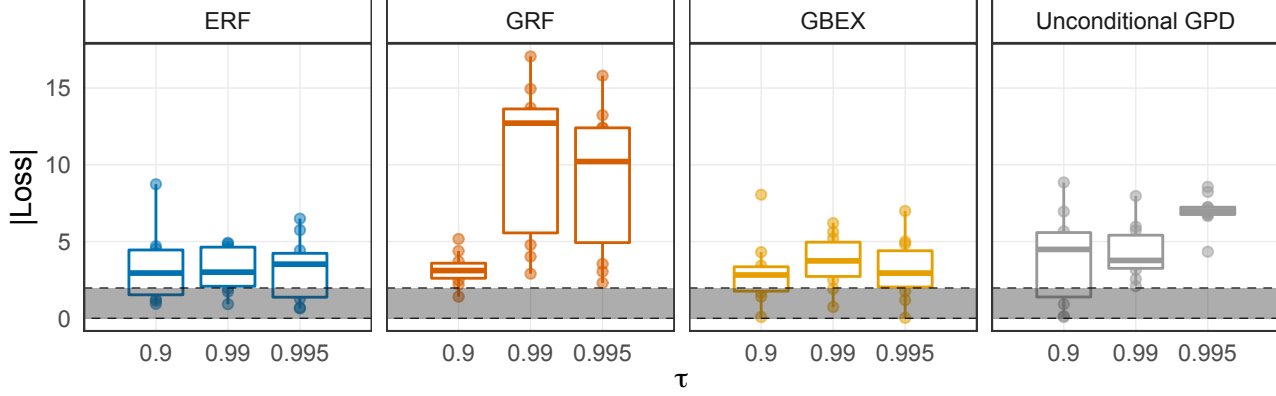


Figure 8: Absolute value of the loss (5.1) for the different methods fitted on the original response of the U.S. wage data. The shaded area represents the 95% interval of the absolute value of a standard normal distribution.

## A Proof of Theorem 1

Given the data generating process of Assumption 1 in the main text, define the random variable  $Z = (Y - Q_X(\tau_0))_+$ . We then have the stochastic representation

$$(X, Z, 1\{Z > 0\}) \stackrel{d}{=} (X, VP, P), \quad (\text{A.1})$$

where  $V$  follows a GPD with parameter vector  $\theta(X)$ , and  $P \sim \text{Bernoulli}(1 - \tau_0)$ , independent of  $X$  and  $V$ . Similarly, for the training data  $(X_i, Y_i)$  we may use an analogous representation with  $(X_i, V_i P_i, P_i)$  as in (A.1),  $i = 1, \dots, n$ . With this we can rewrite the weighted (negative) log-likelihood function in (3.3) as

$$L_n(\theta; x) = \sum_{i=1}^n w_n(x, X_i) \ell_\theta(V_i) P_i,$$

Moreover, for a fixed predictor value  $x \in \text{Int } \mathcal{X}$  let  $V^*$  denote a GPD with parameter vector  $\theta(x)$  and define  $L(\theta; x) = \mathbb{E}[\ell_\theta(V^*)P]$ , where  $\theta \in (0, \infty)^2$ . To prove our result we rely on Theorem 5.7 of [van der Vaart \(1998\)](#), which we state here adapted to our setting.

**Theorem 2.** *Let  $\theta \mapsto L_n(\theta; x)$  be random functions, and let  $\theta \mapsto L(\theta; x)$  be a fixed function such that, for  $x \in \text{Int } \mathcal{X}$ , it holds*

$$\sup_{\theta \in \Theta} |L_n(\theta; x) - L(\theta; x)| \xrightarrow{\mathbb{P}} 0, \quad (\text{A.2})$$

$$L(\theta(x); x) < \inf \left\{ L(\theta; x) : \|\theta - \theta(x)\|_2 \geq \delta, \theta \in \Theta \right\}, \text{ for all } \delta > 0. \quad (\text{A.3})$$

*Then any sequence of estimators  $\hat{\theta}(x)$  with  $L_n(\hat{\theta}(x); x) \leq L_n(\theta(x); x) + o_P(1)$  converges in probability to  $\theta(x)$ .*

We can now prove our Theorem 1.

*Proof of Theorem 1.* First, notice that  $\theta(x) \in \theta(X) \subset \Theta$ , where  $\Theta$  is compact. Therefore, from (3.4) in the main text, we have that  $L_n(\hat{\theta}(x); x) \leq L_n(\theta(x); x)$  for all  $n > 0$ . Furthermore, a standard argument using Kullback–Leibler divergence implies the true parameter  $\theta(x)$  is a minimizer for  $\theta \mapsto L(\theta; x)$ . Since the GPD is identifiable, the true parameter is a unique minimizer, satisfying condition (A.3). Moreover, from Lemma 1, condition (A.2) is satisfied.

Therefore, from Theorem 2, the estimator  $\hat{\theta}(x) \rightarrow \theta(x)$  in probability as  $n \rightarrow \infty$ .  $\square$

**Lemma 1.** *Under the assumptions of Theorem 1, it holds that  $\sup_{\theta \in \Theta} |L_n(\theta; x) - L(\theta; x)| \xrightarrow{\mathbb{P}} 0$ .*

*Proof.* We have that

$$\begin{aligned} L_n(\theta; x) &= \sum_{i=1}^n w_n(x, X_i) \ell_{\theta}(V_i) P_i \\ &= \sum_{i=1}^n w_n(x, X_i) \ell_{\theta}(V_i^*) P_i + \sum_{i=1}^n w_n(x, X_i) (\ell_{\theta}(V_i) - \ell_{\theta}(V_i^*)) P_i \\ &= S_{1,n}(\theta) + S_{2,n}(\theta), \end{aligned}$$

where we couple the random variables  $V_i$  and  $V_i^*$  through  $V_i = F_{\theta(X_i)}^{-1}(U_i)$ ,  $V_i^* = F_{\theta(x)}^{-1}(U_i)$ ,  $U_i \stackrel{iid}{\sim} \text{Unif}[0, 1]$ , and  $F_{\theta}^{-1}$  is the inverse of the GPD function with parameter  $\theta \in \Theta$ . By Lemma 2 and 6, the claim follows.  $\square$

**Lemma 2.** *Under the assumptions of Theorem 1, it holds that  $\sup_{\theta \in \Theta} |S_{1,n}(\theta) - L(\theta; x)| \xrightarrow{\mathbb{P}} 0$ .*

*Proof.* Corollary 2.2 of Newey (1991) provides sufficient conditions for uniform convergence.

1. (Compactness):  $\Theta$  is compact.
2. (Pointwise convergence): For each  $\theta \in \Theta$ ,  $S_{1,n}(\theta) - L(\theta; x) = o_P(1)$ .
3. (Stochastic Equicontinuity): There exists  $C_n = O_P(1)$  such that for all  $\theta, \theta' \in \Theta$ ,  $|S_{1,n}(\theta) - S_{1,n}(\theta')| \leq C_n \|\theta - \theta'\|_2$ .
4. (Continuity): The map  $\theta \mapsto L(\theta; x)$  is continuous.

Condition 1 holds by assumption. The remaining conditions are shown in Lemmas 3, 4, and 5, respectively.  $\square$

**Lemma 3.** *For each  $\theta \in \Theta$ , it holds that  $S_{1,n}(\theta) - L(\theta; x) = o_P(1)$ .*

*Proof.* For each  $\theta \in \Theta$ , recall that  $L(\theta; x) = \mathbb{E}[\ell_{\theta}(V^*)P]$ , where  $V^* \sim \text{GPD}(\theta(x))$ . Furthermore, we have that

$$S_{1,n}(\theta) = \sum_{i=1}^n w_n(x, X_i) \ell_{\theta}(V_i^*) P_i = \frac{1}{B} \sum_{b=1}^B \sum_{i=1}^n w_{n,b}(x, X_i) \ell_{\theta}(V_i^*) P_i = \frac{1}{B} \sum_{b=1}^B T_{n,b}(x, \theta),$$

where  $T_{n,b}(x, \theta)$  is the output of a regression gradient tree (Athey et al., 2019) with response  $\ell_\theta(V_i^*)P_i$  independent of  $w_{n,b}(x, X_i)$ ,  $i = 1, \dots, n$ . Consider a tree  $T_{n,b}(x, \theta)$ ,  $b = 1, \dots, B$ , of the generalized random forest. Its expectation writes

$$\begin{aligned}\mathbb{E}(T_{n,b}(x, \theta)) &= \sum_{i=1}^n \mathbb{E}(w_{n,b}(x, X_i) \ell_\theta(V_i^*) P_i) = \sum_{i=1}^n \mathbb{E}(w_{n,b}(x, X_i)) \mathbb{E}(\ell_\theta(V_i^*) P_i) \\ &= \mathbb{E} \left\{ \sum_{i=1}^n w_{n,b}(x, X_i) \right\} \mathbb{E}(\ell_\theta(V^*) P) = \mathbb{E}(\ell_\theta(V^*) P) = L(\theta; x),\end{aligned}\tag{A.4}$$

since the weights sum to one. Therefore,  $\mathbb{E}(S_{1,n}(\theta)) = L(\theta; x)$ . Concerning the variance of the thinning  $\ell_\theta(V^*)P$  we have that

$$V(\ell_\theta(V^*)P) = \mathbb{E}(\ell_\theta(V^*)^2) \mathbb{E}(P^2) - \mathbb{E}(\ell_\theta(V^*))^2 \mathbb{E}(P)^2 < +\infty,\tag{A.5}$$

since  $P$  is a Bernoulli variable and  $\ell_\theta(V^*)$  has exponential tail. Therefore, the variance of  $T_{n,b}(x, \theta)$  writes

$$\begin{aligned}\mathbb{V}(T_{n,b}(x, \theta)) &= \mathbb{E} \left\{ (T_{n,b}(x, \theta) - L(\theta; x))^2 \right\} = \mathbb{E} \left\{ \left( \sum_{i=1}^n w_{n,b}(x, X_i) (\ell_\theta(V_i^*) P_i - L(\theta; x)) \right)^2 \right\} \\ &= \mathbb{E} \left( \sum_{i=1}^n w_{n,b}(x, X_i)^2 (\ell_\theta(V_i^*) P_i - L(\theta; x))^2 \right. \\ &\quad \left. + \sum_{i \neq j} w_{n,b}(x, X_i) w_{n,b}(x, X_j) (\ell_\theta(V_i^*) P_i - L(\theta; x)) (\ell_\theta(V_j^*) P_j - L(\theta; x)) \right) \\ &= \mathbb{V}(\ell_\theta(V^*) P) \mathbb{E} \left( \sum_{i=1}^n w_{n,b}(x, X_i)^2 \right) \leq \mathbb{V}(\ell_\theta(V^*) P) < +\infty,\end{aligned}\tag{A.6}$$

where the fourth equality holds because  $(V_i^*, P_i)$  are i.i.d., the second last inequality holds because  $0 \leq w_{n,b}(x, X_i) \leq 1$ , and the last inequality follows from (A.5). Using results about  $U$ -statistics (Hoeffding, 1948), Wager and Athey (2018) show that the variance of a forest is at most  $s/n$  times the variance of a tree, that is

$$\limsup_{n \rightarrow \infty} \frac{n}{s} \frac{\mathbb{V}(S_{1,n}(\theta))}{\mathbb{V}(T_{n,b}(x, \theta))} \leq 1.\tag{A.7}$$

where  $s < n$  denotes the subsample size. From Assumption 3, we have that  $s/n \rightarrow 0$ , therefore (A.6) and (A.7) imply that  $\mathbb{V}(S_{1,n}(\theta)) \rightarrow 0$  as  $n \rightarrow \infty$ . The result follows from Markov's inequality.  $\square$

**Lemma 4.** *There exists  $C_n = O_P(1)$  such that for all  $\theta, \theta' \in \Theta$ ,  $|S_{1,n}(\theta) - S_{1,n}(\theta')| \leq C_n \|\theta - \theta'\|_2$ .*

*Proof.* The negative log-likelihood  $\theta \mapsto \ell_\theta(z)$  is defined for each  $z \geq 0$  and  $\theta \in (0, \infty)^2$  as

$$\ell_\theta(z) = \log \sigma + \left(1 + \frac{1}{\xi}\right) \log \left(1 + \frac{\xi}{\sigma} z\right).$$

Therefore, its partial derivatives can be bounded by

$$\begin{aligned} |\partial_\xi \ell_\theta(z)| &\leq \frac{1}{\xi^2} \log \left(1 + \frac{\xi}{\sigma} z\right) + \frac{1 + \frac{1}{\xi}}{\xi}, \\ |\partial_\sigma \ell_\theta(z)| &\leq \frac{1}{\sigma} + \frac{1 + \frac{1}{\xi}}{\sigma}, \end{aligned} \tag{A.8}$$

for any  $\theta = (\sigma, \xi) \in (0, \infty)^2$ . The bounds from (A.8) are continuous on the compact set  $\Theta \subset (0, \infty)^2$ , and therefore, from an application of the dominated convergence theorem,

$$g(z) := \sup \{|\partial_\xi \ell_\theta(z)| : \theta \in \Theta\} + \sup \{|\partial_\sigma \ell_\theta(z)| : \theta \in \Theta\} \tag{A.9}$$

is integrable with respect to a GPD with parameter vector  $\theta(x)$ . Moreover, for any  $\theta, \theta' \in \Theta$ , the mean-value theorem and the Cauchy–Schwarz inequality imply

$$|\ell_\theta(z) - \ell_{\theta'}(z)| = |\nabla \ell_{\tilde{\theta}}(z)(\theta - \theta')| \leq \|\nabla \ell_{\tilde{\theta}}(z)\|_2 \|\theta - \theta'\|_2, \tag{A.10}$$

where  $\tilde{\theta} = c\theta + (1 - c)\theta'$  for some  $0 < c < 1$ , and  $z \geq 0$ . Furthermore, from (A.9), we have that

$$\|\nabla \ell_{\tilde{\theta}}(z)\|_2 \leq |\partial_\xi \ell_{\tilde{\theta}}(z)| + |\partial_\sigma \ell_{\tilde{\theta}}(z)| \leq g(z). \tag{A.11}$$

From equations (A.10) and (A.11) it follows that  $\ell_\theta(z)$  is Lipschitz in  $\theta \in \Theta$  with constant  $g(z)$ ,  $z \geq 0$ . Therefore,

$$\begin{aligned} |S_{1,n}(\theta) - S_{1,n}(\theta')| &= \left| \sum_{i=1}^n w_n(x, X_i) (\ell_\theta(V_i^*) - \ell_{\theta'}(V_i^*)) P_i \right| \leq \sum_{i=1}^n w_n(x, X_i) P_i |\ell_\theta(V_i^*) - \ell_{\theta'}(V_i^*)| \\ &\leq \left( \sum_{i=1}^n w_n(x, X_i) g(V_i^*) P_i \right) \|\theta - \theta'\|_2 =: C_n \|\theta - \theta'\|_2. \end{aligned}$$

For every  $n \in \mathbb{N}$  and  $i = 1, \dots, n$ ,  $V_i^*$  is independent of  $w_n(x, X_i)$  and  $P_i$ . Therefore, since  $z \mapsto g(z)$  is integrable with respect to a GPD with parameter vector  $\theta(x)$  it follows that  $\mathbb{E}[C_n] < +\infty$ . Hence,  $C_n = O_P(1)$ .  $\square$

**Lemma 5.** *The map  $\theta \mapsto L(\theta; x)$  is continuous.*

*Proof.* For any  $\theta \in \Theta$ , recall that

$$L(\theta; x) = \mathbb{E}[\ell_\theta(V^*)P] = \left\{ \log \sigma + \left(1 + \frac{1}{\xi}\right) \mathbb{E} \left[ \log \left[ 1 + \frac{\xi}{\sigma} V^* \right] \right] \right\} (1 - \tau_0).$$

The maps  $\theta \mapsto \log \sigma$  and  $\theta \mapsto (1 + 1/\xi)$  are continuous for  $\theta \in \Theta$ . Also, by an application of the dominated convergence theorem, the map  $\theta \mapsto \mathbb{E} \left[ \log \left( 1 + \frac{\xi}{\sigma} V^* \right) \right]$  is continuous for  $\theta \in \Theta$ .  $\square$

**Lemma 6.** *Under the assumptions of Theorem 1, it holds that  $\sup_{\theta \in \Theta} |S_{2,n}(\theta)| \xrightarrow{\mathbb{P}} 0$ .*

*Proof.* We have that

$$\begin{aligned} 0 &\leq \sup_{\theta \in \Theta} |S_{2,n}(\theta)| = \sup_{\theta \in \Theta} \left| \sum_{i=1}^n w_n(x, X_i) P_i \left( \ell_\theta \circ F_{\theta(X_i)}^{-1}(U_i) - \ell_\theta \circ F_{\theta(x)}^{-1}(U_i) \right) \right| \\ &\leq \sup_{\theta \in \Theta} \sum_{i=1}^n w_n(x, X_i) P_i \left| \ell_\theta \circ F_{\theta(X_i)}^{-1}(U_i) - \ell_\theta \circ F_{\theta(x)}^{-1}(U_i) \right| \\ &\leq \sup_{\theta \in \Theta} \sum_{i=1}^n w_n(x, X_i) P_i K(\theta, U_i) \|X_i - x\|_2 \\ &\leq \sup \left\{ \|X_i - x\|_2 : w_n(x, X_i) > 0, i = 1, \dots, n \right\} \sum_{i=1}^n w_n(x, X_i) P_i \sup_{\theta \in \Theta} K(\theta, U_i) \\ &= o_P(1), \end{aligned} \tag{A.12}$$

where the second last inequality follows from Lemma 7.a) and the last equality follows from Lemmas 8 and 7.b).  $\square$

**Lemma 7.** *Let  $x \in \text{Int } \mathcal{X}$ ,  $U \sim \text{Unif}[0, 1]$ , and  $\theta \in \Theta$ .*

*a) Then, there exists a function  $K(\theta, U) < +\infty$  such that for any  $y \in \mathcal{X}$ ,*

$$\left| \ell_\theta \circ F_{\theta(y)}^{-1}(U) - \ell_\theta \circ F_{\theta(x)}^{-1}(U) \right| \leq K(\theta, U) \|y - x\|_2.$$

*b) Then, under the assumptions of Theorem 1, it holds that*

$$\sum_{i=1}^n w_n(x, X_i) P_i \sup_{\theta \in \Theta} K(\theta, U_i) = O_P(1).$$

*Proof.*

*a)* Let  $U \sim \text{Unif}[0, 1]$ , and  $\theta \in \Theta$ . For any  $y \in \mathcal{X}$  define

$$g(y; \theta, W) := \ell_\theta \circ F_{\theta(y)}^{-1}(1 - 1/W) = \log \sigma + \left(1 + \frac{1}{\xi}\right) \log \left( 1 + \frac{\xi}{\sigma} \frac{\sigma(y)}{\xi(y)} \left\{ W^{\xi(y)} - 1 \right\} \right), \tag{A.13}$$

where  $W := 1/(1 - U) \sim \text{Pareto}(1)$  with support  $[1, \infty)$ . The map  $y \mapsto g(y; \theta, W)$  admits partial derivatives with respect to  $y_j$ ,  $j = 1, \dots, p$ , i.e.,

$$\begin{aligned} \partial_{y_j} g(y; \theta, W) &= \left(1 + \frac{1}{\xi}\right) \left(1 + \frac{\xi}{\sigma} \frac{\sigma(y)}{\xi(y)} \left\{W^{\xi(y)} - 1\right\}\right)^{-1} \frac{\xi}{\sigma} \\ &\quad \times \left( \frac{\sigma'_j(y)\xi(y) - \sigma(y)\xi'_j(y)}{\xi(y)^2} \left\{W^{\xi(y)} - 1\right\} + \frac{\sigma(y)}{\xi(y)} \left\{W^{\xi(y)} \log W\right\} \xi'_j(y) \right), \end{aligned} \quad (\text{A.14})$$

where  $\sigma'_j$ , and  $\xi'_j$  are the  $j$ th partial derivatives of  $y \mapsto \sigma(y)$  and  $y \mapsto \xi(y)$ , respectively. From Assumption 2 in the main text, we know that  $y \mapsto \partial_{y_j} g(y; \theta, W)$  are continuous on the interior of  $\mathcal{X}$ . Thus, for  $x \in \text{Int } \mathcal{X}$  and  $y \in \mathcal{X}$ , the mean-value theorem and the Cauchy–Schwarz inequality imply

$$|g(y; \theta, W) - g(x; \theta, W)| \leq \|\nabla g(x'; \theta, W)\|_2 \|y - x\|_2,$$

where  $x' = cy + (1 - c)x$  for some  $c \in (0, 1)$ . Moreover, Assumption 2 ensures that the partials derivatives of  $y \mapsto g(y; \theta, W)$  exist on the compact set  $\mathcal{X}$ . Thus, we can define  $K(\theta, U) := \sum_{j=1}^p \sup\{|\partial_{y_j} g(y; \theta, W)| : y \in \mathcal{X}\}$  and obtain

$$\left| \ell_\theta \circ F_{\theta(y)}^{-1}(U) - \ell_\theta \circ F_{\theta(x)}^{-1}(U) \right| \leq K(\theta, U) \|y - x\|_2.$$

**b)** From Part a), we have that  $K(\theta, U) = \sum_{j=1}^p \sup\{|\partial_{y_j} g(y; \theta, W)| : y \in \mathcal{X}\}$ , where  $\theta \in \Theta$ , and  $W \geq 1$  follows a standard Pareto distribution. For every  $j = 1, \dots, p$  it holds that

$$\begin{aligned} \sup_{y \in \mathcal{X}} |\partial_{y_j} g(y; \theta, W)| &\leq \sup_{y \in \mathcal{X}} \left(1 + \frac{1}{\xi}\right) \left(1 + \frac{\xi}{\sigma} \frac{\sigma(y)}{\xi(y)} \left\{W^{\xi(y)} - 1\right\}\right)^{-1} \frac{\xi}{\sigma} \\ &\quad \times \left( \frac{|\sigma'_j(y)\xi(y) - \sigma(y)\xi'_j(y)|}{\xi(y)^2} \left\{W^{\xi(y)} - 1\right\} + \frac{\sigma(y)}{\xi(y)} |\xi'_j(y)| \left\{W^{\xi(y)} \log W\right\} \right) \\ &=: \sup_{y \in \mathcal{X}} \left(1 + \frac{1}{\xi}\right) \frac{\xi}{\sigma} \left( \frac{M_{1j}(y) \left\{W^{\xi(y)} - 1\right\}}{1 + M(y, \theta) \left\{W^{\xi(y)} - 1\right\}} + \frac{M_{2j}(y) \left\{W^{\xi(y)} \log W\right\}}{1 + M(y, \theta) \left\{W^{\xi(y)} - 1\right\}} \right), \end{aligned}$$

where  $M_{1j}(y) = |\sigma'_j(y)\xi(y) - \sigma(y)\xi'_j(y)|/\xi(y)^2 \geq 0$ ,  $M_{2j}(y) = \sigma(y)|\xi'_j(y)|/\xi(y) \geq 0$ , and  $M(y, \theta) = (\sigma(y)\xi)/(\xi(y)\sigma) > 0$ . Notice that almost surely

$$\begin{aligned} 0 &\leq \frac{M_{1j}(y) \left\{W^{\xi(y)} - 1\right\}}{1 + M(y, \theta) \left\{W^{\xi(y)} - 1\right\}} \leq \frac{M_{1j}(y)}{M(y, \theta)}, \\ 0 &\leq \frac{M_{2j}(y) W^{\xi(y)}}{1 + M(y, \theta) \left\{W^{\xi(y)} - 1\right\}} \leq \max \left\{ M_{2j}(y), \frac{M_{2j}(y)}{M(y, \theta)} \right\}. \end{aligned}$$



Therefore, for every  $j = 1, \dots, p$ , we have

$$\begin{aligned} \sup_{\theta \in \Theta, y \in \mathcal{X}} |\partial_{y_j} g(y; \theta, W)| &\leq \sup_{\theta \in \Theta, y \in \mathcal{X}} \left( 1 + \frac{1}{\xi} \right) \frac{\xi}{\sigma} \left( \frac{M_{1j}(y)}{M(y, \theta)} + \max \left\{ M_{2j}(y), \frac{M_{2j}(y)}{M(y, \theta)} \right\} \log W \right) \\ &\leq \left( 1 + \frac{1}{\xi^-} \right) \frac{\xi^+}{\sigma^-} \left( \frac{M_{1j}}{M} + \max \left\{ M_{2j}, \frac{M_{2j}}{M} \right\} \log W \right) \\ &= \left( 1 + \frac{1}{\xi^-} \right) \frac{\xi^+}{\sigma^-} \left( \frac{M_{1j}}{M} + \frac{M_{2j}}{M} \log W \right), \end{aligned}$$

where  $M_{hj} := \sup\{M_{hj}(y) : y \in \mathcal{X}\}$ , for  $h = 1, 2$ ,  $M := \inf\{M(y, \theta) : \theta \in \Theta, y \in \mathcal{X}\} < 1$ , and  $\sigma^+$ ,  $\xi^+$  ( $\sigma^-$ ,  $\xi^-$ ) are the maxima (minima) of the parameter values over the compact set  $\Theta$ , respectively. Since  $W \sim \text{Pareto}(1)$  with support  $[1, \infty)$ , it follows that  $\log W \sim \text{Exp}(1)$ . Therefore, by taking expectation we obtain

$$\mathbb{E} \left( \sup_{\theta \in \Theta} K(\theta, U) \right) \leq \left( 1 + \frac{1}{\xi^-} \right) \frac{\xi^+}{\sigma^-} \sum_{j=1}^p \left( \frac{M_{1j} + M_{2j}}{M} \right) =: M^* < \infty.$$

Let  $\varepsilon > 0$  and consider  $M_\varepsilon = (M^* + 1)/\varepsilon > 0$ . Then, for any  $n \in \mathbb{N}$ , it holds that

$$\begin{aligned} \mathbb{P} \left( \sum_{i=1}^n w_n(x, X_i) P_i \sup_{\theta \in \Theta} K(\theta, U_i) > M_\varepsilon \right) &\leq \frac{\mathbb{E} \left( \sum_{i=1}^n w_n(x, X_i) P_i \sup_{\theta \in \Theta} K(\theta, U_i) \right)}{M_\varepsilon} \\ &= \frac{\sum_{i=1}^n \mathbb{E}(w_n(x, X_i)) \mathbb{E}(\sup_{\theta \in \Theta} K(\theta, U_i)) \mathbb{E}(P_i)}{M_\varepsilon} = \frac{\mathbb{E} \left( \sum_{i=1}^n w_n(x, X_i) \right) \mathbb{E}(\sup_{\theta \in \Theta} K(\theta, U)) \mathbb{E}(P)}{M_\varepsilon} \\ &= \frac{\mathbb{E}(\sup_{\theta \in \Theta} K(\theta, U)) (1 - \tau_0)}{M_\varepsilon} \leq \frac{M^* (1 - \tau_0)}{M_\varepsilon} < \varepsilon. \end{aligned}$$

□

**Lemma 8.** *Under the assumptions of Theorem 1, it holds that*

$$\sup \{ \|X_i - x\|_2 : w_n(x, X_i) > 0, i = 1, \dots, n \} = o_P(1).$$

*Proof.* This result follows from Lemma 2 of [Wager and Athey \(2018\)](#) which states that  $\text{diam}(L_b(x)) = o_P(1)$ . It does not require the random forest to be honest; i.e., we can assume that we use the same observations to place the splits and make predictions. For each tree  $b = 1, \dots, B$  of the forest, we subsample  $\mathcal{S}_b \subset \{1, \dots, n\}$  observations from the training data, with  $|\mathcal{S}_b| = s < n$ . Denote by  $L_b(x) \subset \mathcal{X}$  the leaf containing the fixed predictor value  $x \in \mathcal{X}$ . Define the diameter  $\text{diam}(L_b(x)) := \sup_{z, y \in L_b(x)} \|z - y\|_2$  of the leaf  $L_b(x)$  as the length of the longest segment contained inside  $L_b(x)$ . Recall that the weights of a (not necessarily honest) random forest are defined as

$$w_n(x, X_i) = \frac{1}{B} \sum_{b=1}^B w_{n,b}(x, X_i) = \frac{1}{B} \sum_{b=1}^B \frac{\mathbb{1}\{X_i \in L_b(x), i \in \mathcal{S}_b\}}{|\{X_i \in L_b(x), i \in \mathcal{S}_b\}|}.$$

Also, note that

$$\begin{aligned} \{\|X_i - x\|_2 : w_n(x, X_i) > 0, i = 1, \dots, n\} &= \{\|X_i - x\|_2 : \exists b = 1, \dots, B, X_i \in L_b(x), i \in \mathcal{S}_b\} \\ &= \cup_{b=1}^B \{\|X_i - x\|_2 : X_i \in L_b(x), i \in \mathcal{S}_b\} \subset \cup_{b=1}^B \{\|y - x\|_2 : y \in L_b(x)\}. \end{aligned}$$

Therefore,

$$\begin{aligned} \sup \{\|X_i - x\|_2 : w_n(x, X_i) > 0, i = 1, \dots, n\} &\leq \sup \cup_{b=1}^B \{\|y - x\|_2 : y \in L_b(x)\} \\ &= \max_{b=1}^B \sup \{\|y - x\|_2 : y \in L_b(x)\} \leq \max_{b=1}^B \text{diam}(L_b(x)). \end{aligned}$$

Thus, for every  $\varepsilon > 0$

$$\begin{aligned} 0 &\leq \mathbb{P} \left( \sup \{\|X_i - x\|_2 : w_n(x, X_i) > 0, i = 1, \dots, n\} > \varepsilon \right) \\ &\leq \mathbb{P} \left( \max_{b=1}^B \text{diam}(L_b(x)) > \varepsilon \right) \leq \sum_{b=1}^B \mathbb{P} (\text{diam}(L_b(x)) > \varepsilon) \rightarrow 0. \end{aligned}$$

□

## B Partial Derivative on the Boundary

For any function  $f : [0, 1]^p \rightarrow \mathbb{R}$ , we define the first order partial derivative on the boundary by

$$\partial_{x_j} f(x) := \begin{cases} \lim_{h \downarrow 0} \frac{f(x + he_j) - f(x)}{h}, & \text{if } x \in [0, 1]^p, x_j = 0, \\ \lim_{h \downarrow 0} \frac{f(x) - f(x - he_j)}{h}, & \text{if } x \in [0, 1]^p, x_j = 1. \end{cases}$$

## C Weight Function Estimation

In quantile regression tasks, the weight function  $(x, y) \mapsto w_n(x, y)$  estimated by GRF measures the similarity between  $x$  and  $y$  according to their conditional distribution.

Figure 9 shows the localizing weights  $w_n(x, X_i)$ ,  $x, X_i \in \mathbb{R}^p$ , for two test predictors  $x$  with  $x_1 = -0.2, 0.5$ , respectively. The data is generated according to Example 1, with  $n = 2000$  observations and  $p = 40$  predictors. In the left panel of Figure 9, the observations  $(X_i, Y_i)$  with  $X_{i1} < 0$  are the ones influencing most the test predictor  $x$  with  $x_1 = -0.2$ . This is because they share the same conditional distribution. A similar argument holds for the right panel of Figure 9.

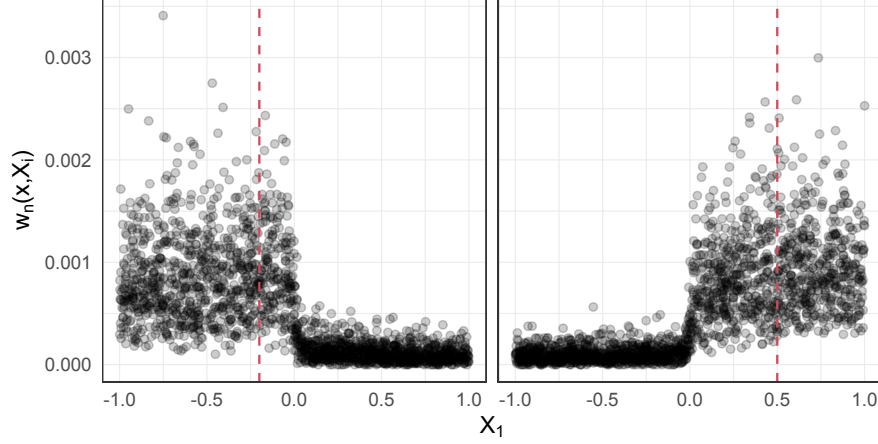


Figure 9: The height of the points represents the localizing weights  $w_n(x, X_i)$  between a test predictor  $x \in \mathbb{R}^p$  and each training observation  $X_i \in \mathbb{R}^p$ . The dashed line indicates the first coordinate of the test predictor values.

## D Additional Material for Simulation Study

### D.1 Sensitivity of Intermediate Threshold Level

Figure 10 shows the square root MISE of predicted quantiles as a function of the intermediate threshold  $\tau_0$  for different quantile levels  $\tau$  and different shape parameters  $\xi$  of the noise variable. Even though the threshold choice has an influence on the prediction accuracy, from the scales of the square root MISE it can be seen that this influence is not too strong. The optimal choice will depend on the properties of the data such as the tail heaviness of the response; for details see [de Haan and Ferreira \(2006, Section 3.2\)](#). In applications, there are numerous data-driven methods for choosing the threshold such as the mean excess plot (see [Embrechts et al., 2012, Section 6.2.2](#)).

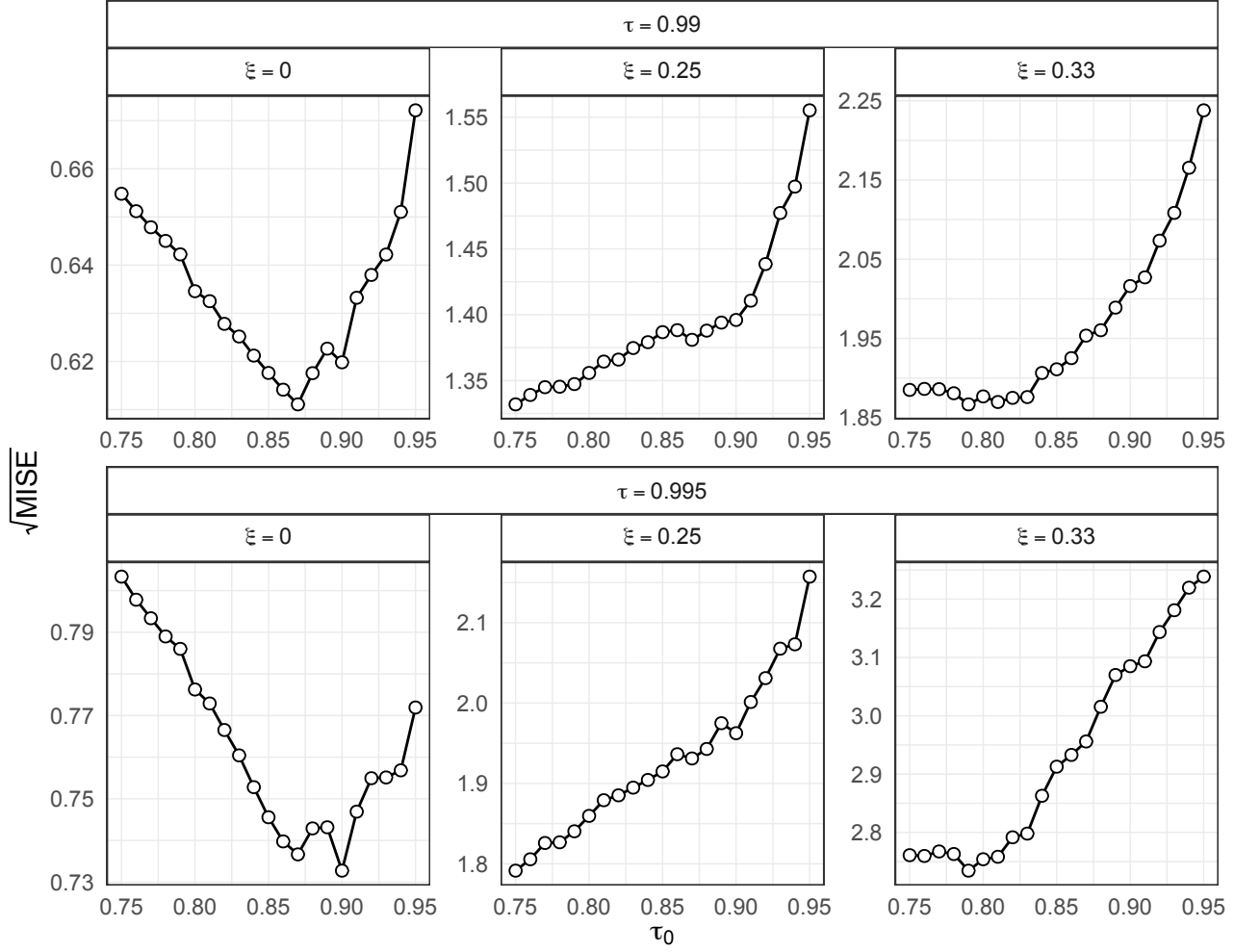


Figure 10: Square root MISE of predicted quantiles as a function of the intermediate threshold  $\tau_0$  for different quantile levels  $\tau$  and different shape parameters  $\xi$  of the noise variable. Each point is an average over  $m = 100$  repetitions. The data is generated according to Example 1 in the main text, where we set the dimension of the predictor space to  $p = 5$ .

## D.2 Experiment 3

In the last experiment mentioned in Section 4, we consider more complex regression functions depending on more signal variables both in the scale and shape parameters. While the predictor variables  $X$  are uniform distributed on  $[-1, 1]^p$  with  $p = 10$ , the conditional response follows three different models

$$(Y \mid X = x) \sim s_j(x)T_{\nu(x)}, \quad j = 1, 2, 3,$$

where we allow both degrees of freedom  $\nu(x)$  and the scale  $s_j(x)$  of the Student's  $t$  distribution to depend on the predictors. In particular, we model the degrees of freedom as a decreasing function

of the first predictor as  $\nu(x) = 3[2 + \tanh(-2x_1)]$ , and the different scale functions as

$$\begin{aligned} s_1(x) &= [2 + \tanh(2x_1)](1 + x_2/2), \\ s_2(x) &= 4 - (x_1^2 + 2x_2^2), \\ s_3(x) &= 1 + 2\pi\varphi(2x_1, 2x_2), \end{aligned}$$

where  $\varphi$  denotes a centered bivariate Gaussian density with unit variance and correlation coefficient equal to 0.75. The first scale function  $s_1(x)$  is non-linear with respect to the first predictor and contains an interaction effect between the first two predictors. The function  $s_2(x)$  is quadratic and decreasing in the first two dimensions. The third scale function  $s_3(x)$  is non-linear in the first two predictors and contains an interaction effect. The sample size is  $n = 5000$ .

In this experiment we compare ERF, GRF, GBEX, EGP Tail and the unconditional method. We leave out EGAM because we observed it performs poorly in the scenarios considered here. Figure 11 shows the boxplots of  $\sqrt{\text{ISE}}$  over  $m = 50$  simulations over different models, methods, and quantile levels. For better visualization, we remove large outliers of GRF, QRF, and EGP Tail. We observe that ERF and GBEX generally outperform the other methods over all models and quantile levels, where GBEX has a slight advantage in high quantiles for Models 2 and 3. GRF and QRF seems to deteriorate completely for very large quantiles.

## E Additional Material for U.S. Wage Analysis

### E.1 Additional Figure

Figure 12 shows that estimated GPD parameters  $\hat{\theta}(x)$  for the original response as a function of age for groups with less or more than 15 years of education.

### E.2 Analysis with Log-Transformed Response

Following Angrist et al. (2009), we consider here the natural logarithm of the wage as response variable for quantile regression. We perform the same analysis as in Section 5 again with this log-transformed response since it highlights several interesting properties of the ERF algorithm. Figure 13 shows the GPD parameters  $\hat{\theta}^{\log}(x)$  estimated by ERF as a function of years of education when the response is  $\log(Y)$ . We notice that the log-transformation makes the response lighter-tailed, with estimated shape parameters  $\hat{\xi}^{\log}(x)$  fairly close to 0. The scale parameters  $\hat{\sigma}^{\log}(x)$  still show a certain structure, but they vary on a much smaller scale compared to  $\hat{\sigma}(x)$  estimated on the original response; see Figure 6 in the main text. These observations are consistent with theory since it is well-known that the log-transformation renders heavy-tailed data into light-tailed (Embrechts et al., 2012, Example 3.3.33). Moreover, the shape parameter on the original data then essentially acts as a scale parameter in the GPD approximation of the log-transformed data, explaining the smaller variation of  $\hat{\sigma}^{\log}(x)$ .

Figure 14 in the main text shows the (exponentiated) predicted quantiles  $\exp\{\hat{Q}_x^{\log}(\tau)\}$  of the different methods as a function of years of education when the response is  $\log(Y)$ ; we removed

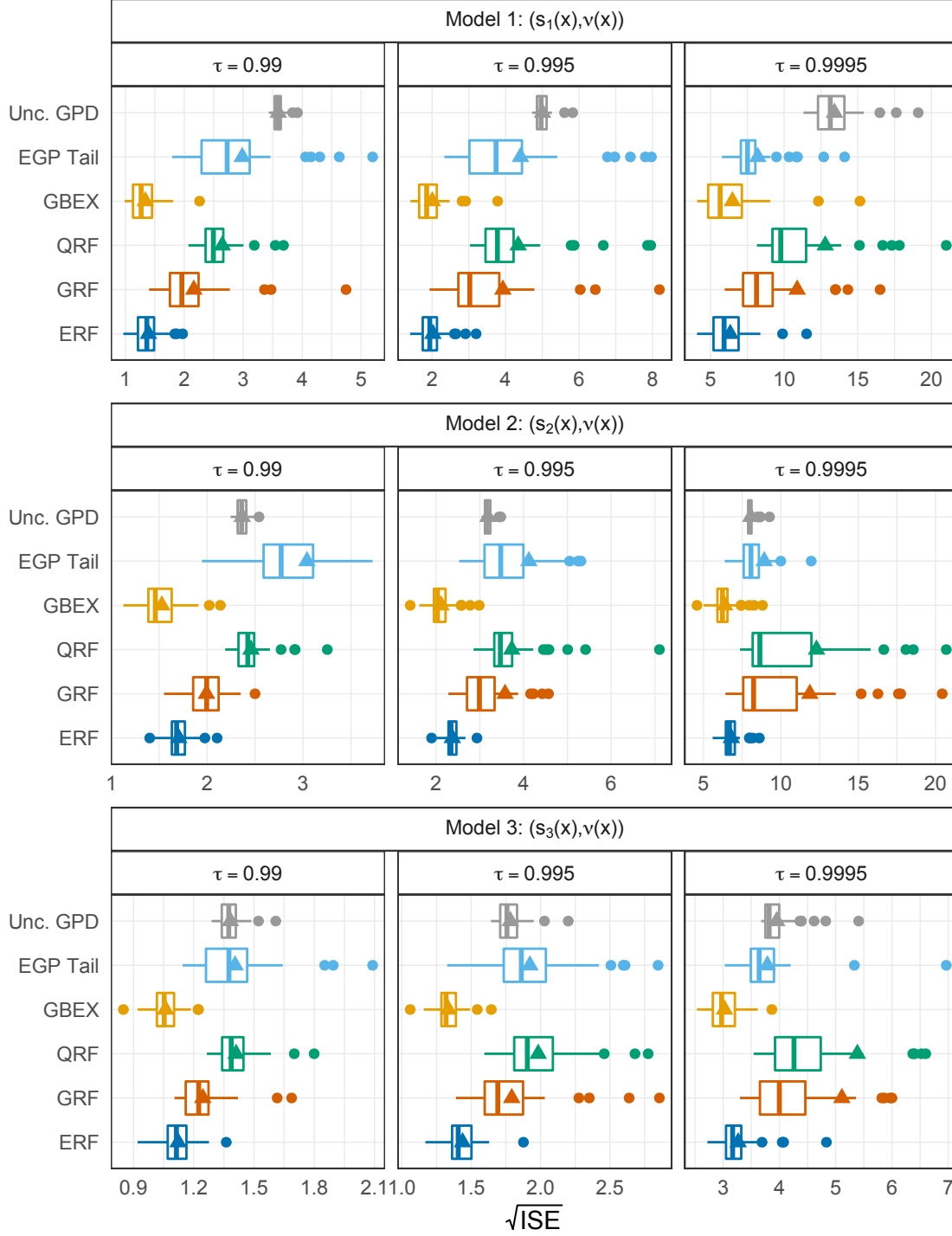


Figure 11: Boxplots of  $\sqrt{\text{ISE}}$  over  $m = 50$  simulations for different generative models (rows) and quantile levels (columns). The predictor space dimension is set to  $p = 10$ . Triangles represent the average values.



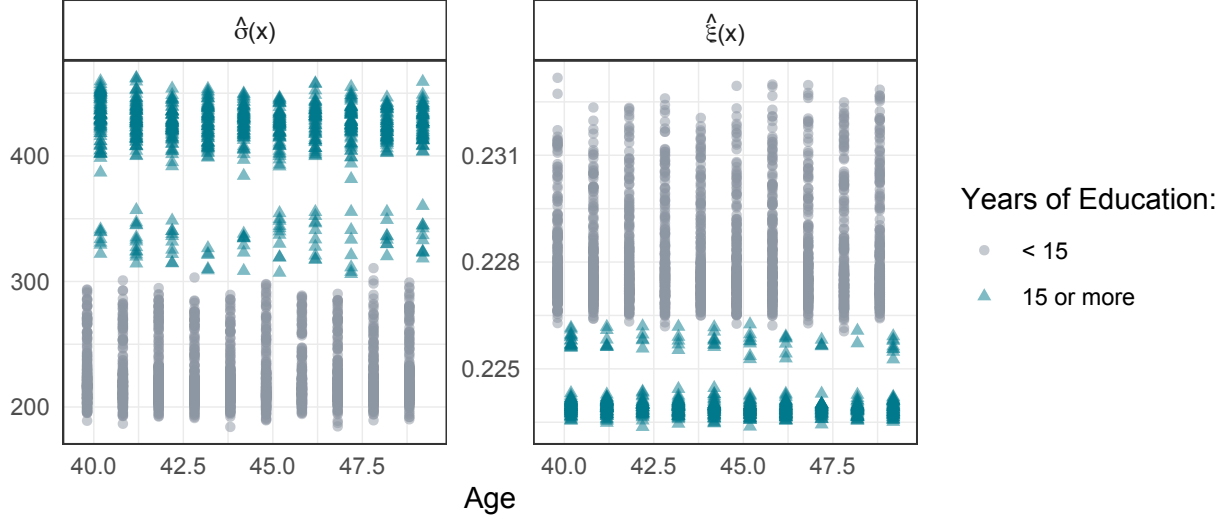


Figure 12: Estimated GPD parameters  $\hat{\theta}(x)$  as a function of age for groups with less (circles) or more (triangles) than 15 years of education.

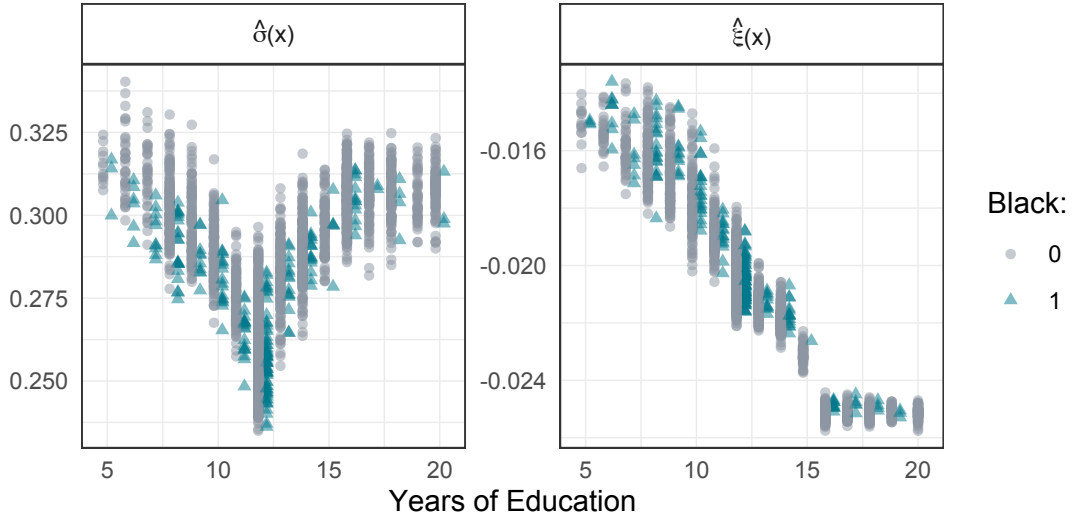


Figure 13: Estimated GPD parameters  $\hat{\theta}(x)$  for the log-response as a function of the years of education for the black (triangles) and white (circles) subgroups.

again all quantiles above 6,000 predicted by GRF. By construction, GRF is invariant to the log-transformation, while the methods based on extrapolation may produce predictions that differ from  $\hat{Q}_x(\tau)$  in Figure 7 fitted on the original data. The reason is that the approximation by the GPD is done on heavy-tailed data on the original scale and on much lighter-tailed data on the log-scale. We observe in Figure 14 that the flexible methods ERF and GBEX have the desirable property that the predictions do not change much under marginal transformations. The unconditional method on the other hand seems to be sensitive to marginal transformation and works better on the log-transformed data as it captures a larger variability of the conditional quantiles even for high  $\tau$ . This is confirmed

by Figure 15 where we observe that the unconditional method has a smaller loss especially for higher quantiles, while all other methods have a similar performance as on the original data. To better understand this behavior, we recall the GPD approximation from (1.1) for large quantiles estimated on the original response as

$$\hat{Q}_x(\tau) \approx \hat{Q}_x(\tau_0) + G^{-1} \left( \frac{\tau - \tau_0}{1 - \tau_0}; \hat{\theta}(x) \right), \quad (\text{E.1})$$

where  $G^{-1}$  is the inverse of the distribution function (2.2) of the GPD; see Figure 7 in the main text. On the other hand, first estimating the quantiles of the log-transformed data with a similar approximation and then exponentiating these estimates results in

$$\exp\{\hat{Q}_x^{\log}(\tau)\} \approx \hat{Q}_x(\tau_0) \exp \left\{ G^{-1} \left( \frac{\tau - \tau_0}{1 - \tau_0}; \hat{\theta}^{\log}(x) \right) \right\}, \quad (\text{E.2})$$

where  $\hat{\theta}^{\log}(x)$  is the parameter vector of the GPD fitted for the response  $\log(Y)$ ; see Figure 14. We note that  $\hat{Q}_x(\tau_0)$  is the same in both approximations since it is fitted using quantile GRF, which is invariant under marginal transformations. Comparing (E.1) and (E.2) shows that the intermediate quantiles have an additive and multiplicative influence on the extreme quantiles, respectively. This explains why using the unconditional method for the GPD with  $\hat{\theta}^{\log}(x) \equiv \hat{\theta}^{\log}$  seems to work better on the log-transformed data. Indeed, the different multiplicative scalings observed for ERF and GBEX in Figure 7 in the main text cannot be represented by (E.1) with unconditional GPD, but they can be represented by (E.2) if the intermediate quantile already carries the structure.

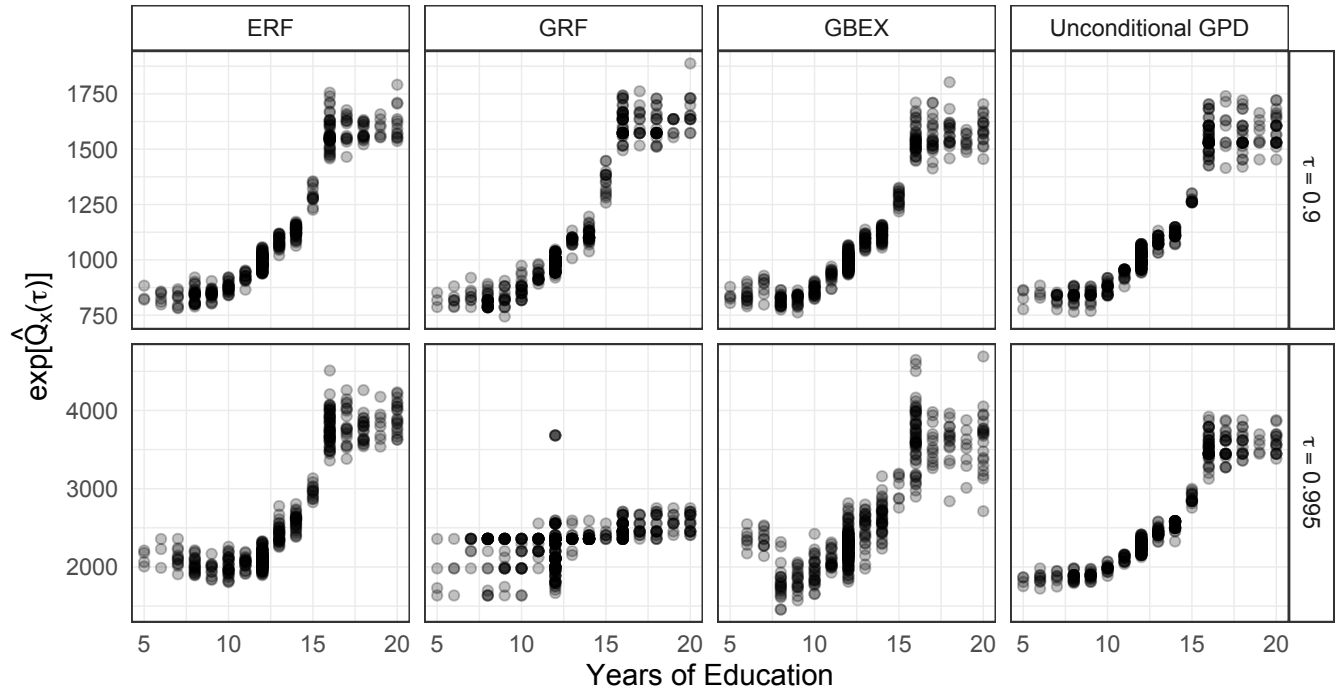


Figure 14: Predicted quantiles at levels  $\tau = 0.9, 0.995$  for ERF, GRF, GBEX, and the unconditional method fitted on the log-response.

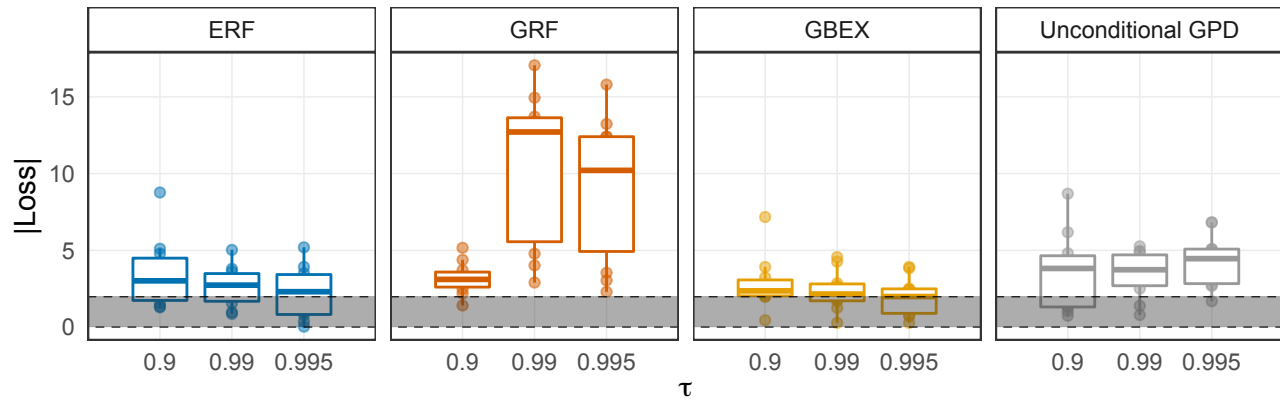


Figure 15: Absolute value of the loss (5.1) for the different methods fitted on the log-response of the U.S. wage data. The shaded area represents the 95% interval of the absolute value of a standard normal distribution.

## References

- J. D. Angrist, V. Chernozhukov, and I. Fernández-Val. Quantile regression under misspecification, with an application to the U.S. wage structure. *Econometrica*, 74(2):539–563, 2006. ISSN 00129682, 14680262. URL <http://www.jstor.org/stable/3598810>.
- J. D. Angrist, V. Chernozhukov, and I. Fernández-Val. Replication data for: Quantile regression under misspecification, with an application to the U.S. wage structure, 2009. URL <https://doi.org/10.7910/DVN/JNEOLQ>. <https://doi.org/10.7910/DVN/JNEOLQ>.
- S. Athey, J. Tibshirani, and S. Wager. Generalized random forests. *The Annals of Statistics*, 47(2): 1148–1178, 2019. URL <https://doi.org/10.1214/18-AOS1709>.
- A. A. Balkema and L. de Haan. Residual Life Time at Great Age. *The Annals of Probability*, 2 (5):792 – 804, 1974. doi: 10.1214/aop/1176996548. URL <https://doi.org/10.1214/aop/1176996548>.
- J. Beirlant, T. D. Wet, and Y. Goegebeur. Nonparametric estimation of extreme conditional quantiles. *Statistical Computation and Simulation*, 74(8):567 – 580, 2004. doi: 10.1080/00949650310001623407. URL <https://doi.org/10.1080/00949650310001623407>.
- J. Beirlant, G. Dierckx, and A. Guillou. Estimation of the extreme-value index and generalized quantile plots. *Bernoulli*, 11(6):949 – 970, 2005. doi: 10.3150/bj/1137421635. URL <https://doi.org/10.3150/bj/1137421635>.
- G. Biau. Analysis of a random forests model. *Journal of Machine Learning Research*, 13(38): 1063–1095, 2012. URL <http://jmlr.org/papers/v13/biau12a.html>.
- L. Breiman. Random forests. *Machine Learning*, 45, 5–32, 2001. ISSN 0885-6125. doi: 10.1023/A:1010933404324. URL <http://dx.doi.org/10.1023/A:1010933404324>.
- A. Bücher and J. Segers. On the maximum likelihood estimator for the generalized extreme-value distribution. *Extremes*, 20(4):839–872, 2017. doi: 10.1007/s10687-017-0292-6. URL <https://doi.org/10.1007/s10687-017-0292-6>.
- A. Bücher, J. Lilienthal, P. Kinsvater, and R. Fried. Penalized quasi-maximum likelihood estimation for extreme value models with application to flood frequency analysis. *Extremes*, pages 1–24, 2020. doi: 10.1007/s10687-020-00379-y. URL <https://doi.org/10.1007/s10687-020-00379-y>.
- V. Chavez-Demoulin and A. C. Davison. Generalized additive modelling of sample extremes. *Journal of the Royal Statistical Society: Series C (Applied Statistics)*, 54(1):207–222, 2005. doi: <https://doi.org/10.1111/j.1467-9876.2005.00479.x>. URL <https://rss.onlinelibrary.wiley.com/doi/abs/10.1111/j.1467-9876.2005.00479.x>.
- V. Chernozhukov. Extremal quantile regression. *The Annals of Statistics*, 33(2):806 – 839, 2005. doi: 10.1214/009053604000001165. URL <https://doi.org/10.1214/009053604000001165>.

- S. G. Coles and M. J. Dixon. Likelihood-based inference for extreme value models. *Extremes*, 2(1):5–23, 1999.
- A. Daouia, L. Gardes, S. Girard, and A. Lekina. Kernel estimators of extreme level curves. *Test, Spanish Society of Statistics and Operations Research/Springer*, 20(2):311 – 333, 2011. doi: 10.1007/s11749-010-0196-0.
- L. de Haan and A. Ferreira. *Extreme Value Theory*. Springer, New York, 2006.
- P. de Zea Bermudez and M. A. Turkman. Bayesian approach to parameter estimation of the generalized pareto distribution. *Test*, 12(1):259–277, 2003.
- C. Dombry. Existence and consistency of the maximum likelihood estimators for the extreme value index within the block maxima framework. *Bernoulli*, 21(1):420 – 436, 2015. doi: 10.3150/13-BEJ573. URL <https://doi.org/10.3150/13-BEJ573>.
- C. Dombry and A. Ferreira. Maximum likelihood estimators based on the block maxima method. *Bernoulli*, 25(3):1690–1723, 2019. ISSN 1350-7265. doi: 10.3150/18-BEJ1032. URL <https://doi.org/10.3150/18-BEJ1032>.
- H. Drees, A. Ferreira, and L. de Haan. On maximum likelihood estimation of the extreme value index. *Ann. Appl. Probab.*, 14(3):1179–1201, 2004. ISSN 1050-5164. doi: 10.1214/105051604000000279. URL <https://doi.org/10.1214/105051604000000279>.
- P. Embrechts, C. Klüppelberg, and T. Mikosch. *Modelling Extremal Events for Insurance and Finance*. Stochastic Modelling and Applied Probability. Springer Heidelberg New York Dordrecht London, 9<sup>th</sup> edition, 2012. ISBN 978-3-540-60931-5. doi: 10.1007/978-3-642-33483-2.
- S. Engelke, R. de Fondeville, and M. Oesting. Extremal behaviour of aggregated data with an application to downscaling. *Biometrika*, 106:127–144, 2019. doi: 10.1093/biomet/asv052.
- S. Farkas, O. Lopez, and M. Thomas. Cyber claim analysis through generalized pareto regression trees with applications to insurance pricing and reserving. Preprint at <https://hal.archives-ouvertes.fr/hal-02118080v2>, 2020.
- A. Ferreira, L. de Haan, and C. Zhou. Exceedance probability of the integral of a stochastic process. *J. Multivariate Anal.*, 105:241 – 257, 2012.
- J. H. Friedman. Greedy function approximation: a gradient boosting machine. *The Annals of Statistics*, 29(5):1189–1232, 2001.
- J. H. Friedman. Stochastic gradient boosting. *Computational Statistics and Data Analysis*, 38(4): 367–378, 2002.
- L. Gardes and G. Stupfler. An integrated functional Weissman estimator for conditional extreme quantiles. *REVSTAT*, 17(1):109–144, 2019. ISSN 1645-6726. doi: 10.1007/s10687-013-0174-5. URL <https://doi.org/10.1007/s10687-013-0174-5>.

- J. H. Halton. Algorithm 247: Radical-inverse quasi-random point sequence. *Commun. ACM*, 7(12):701–702, Dec. 1964. ISSN 0001-0782. doi: 10.1145/355588.365104. URL <https://doi.org/10.1145/355588.365104>.
- T. J. Hastie, R. Tibshirani, and J. Friedman. *The Elements of Statistical Learning*. Springer, New York, NY, USA, second edition, 2009.
- P. J. Heagerty and M. S. Pepe. Semiparametric estimation of regression quantiles with application to standardizing weight for height and age in us children. *Journal of the Royal Statistical Society: Series C (Applied Statistics)*, 48(4):533–551, 1999.
- W. Hoeffding. A Class of Statistics with Asymptotically Normal Distribution. *The Annals of Mathematical Statistics*, 19(3):293 – 325, 1948. doi: 10.1214/aoms/1177730196. URL <https://doi.org/10.1214/aoms/1177730196>.
- R. Koenker. Additive models for quantile regression: Model selection and confidence band-aids. *Brazilian Journal of Probability and Statistics*, 25(3):239 – 262, 2011. doi: 10.1214/10-BJPS131. URL <https://doi.org/10.1214/10-BJPS131>.
- R. Koenker and G. Bassett. Regression quantiles. *Journal of the Econometric Society*, 46(1):33–50, 1978.
- C. Martins-Filho, F. Yao, and M. Torero. High-order conditional quantile estimation based on nonparametric models of regression. *Econometric Reviews*, 34(6 - 10):907 – 958, 2015. doi: 10.1080/07474938.2014.956612.
- N. Meinshausen. Quantile regression forests. *Journal of Machine Learning Research*, 7:983–999, 2006.
- W. K. Newey. Uniform convergence in probability and stochastic equicontinuity. *Econometrica*, 59(4):1161–1167, 1991. ISSN 00129682, 14680262. URL <http://www.jstor.org/stable/2938179>.
- J. I. Pickands. Statistical inference using extreme value order statistics. *Annals of Statistics*, 1975.
- E. Scornet, G. Biau, and J.-P. Vert. Consistency of random forests. *The Annals of Statistics*, 43(4):1716 – 1741, 2015. doi: 10.1214/15-AOS1321. URL <https://doi.org/10.1214/15-AOS1321>.
- R. L. Smith. Maximum likelihood estimation in a class of nonregular cases. *Biometrika*, 72(1): 67–90, 1985. ISSN 00063444. URL <http://www.jstor.org/stable/2336336>.
- R. L. Smith and J. Naylor. A comparison of maximum likelihood and bayesian estimators for the three-parameter weibull distribution. *Journal of the Royal Statistical Society: Series C (Applied Statistics)*, 36(3):358–369, 1987.

- C. J. Stone. Optimal Rates of Convergence for Nonparametric Estimators. *The Annals of Statistics*, 8(6):1348 – 1360, 1980. doi: 10.1214/aos/1176345206. URL <https://doi.org/10.1214/aos/1176345206>.
- C. J. Stone. Optimal Global Rates of Convergence for Nonparametric Regression. *The Annals of Statistics*, 10(4):1040 – 1053, 1982. doi: 10.1214/aos/1176345969. URL <https://doi.org/10.1214/aos/1176345969>.
- M. Taillardat, A.-L. Fougères, P. Naveau, and O. Mestre. Forest-based and semiparametric methods for the postprocessing of rainfall ensemble forecasting. *Weather and Forecasting*, 34(3):617 – 634, 2019. doi: 10.1175/WAF-D-18-0149.1. URL [https://journals.ametsoc.org/view/journals/wefo/34/3/waf-d-18-0149\\_1.xml](https://journals.ametsoc.org/view/journals/wefo/34/3/waf-d-18-0149_1.xml).
- J. W. Taylor. A quantile regression approach to estimating the distribution of multiperiod returns. *The Journal of Derivatives*, 7(1):64–78, 1999. ISSN 1074-1240. doi: 10.3905/jod.1999.319106. URL <https://jod.pm-research.com/content/7/1/64>.
- J. W. Taylor. A quantile regression neural network approach to estimating the conditional density of multiperiod returns. *Journal of Forecasting*, 19(4):299–311, 2000. doi: [https://doi.org/10.1002/1099-131X\(200007\)19:4<299::AID-FOR775>3.0.CO;2-V](https://doi.org/10.1002/1099-131X(200007)19:4<299::AID-FOR775>3.0.CO;2-V). URL <https://onlinelibrary.wiley.com/doi/abs/10.1002/1099-131X%28200007%2919%3A4%3C299%3A%3AAID-FOR775%3E3.0.CO%3B2-V>.
- J. Tibshirani, S. Athey, E. Sverdrup, and S. Wager. *grf: Generalized Random Forests*, 2021. URL <https://CRAN.R-project.org/package=grf>. R package version 2.0.2.
- A. W. van der Vaart. *Asymptotic Statistics*. Cambridge Series in Statistical and Probabilistic Mathematics. Cambridge University Press, 1998. doi: 10.1017/CBO9780511802256.
- J. Velthoen, J.-J. Cai, G. Jongbloed, and M. Schmeits. Improving precipitation forecasts using extreme quantile regression. *Extremes*, 22(4):599–622, 2019.
- J. Velthoen, C. Dombry, J.-J. Cai, and S. Engelke. Gradient boosting for extreme quantile regression. *arXiv preprint arXiv:2103.00808*, 2021.
- S. Wager and S. Athey. Estimation and inference of heterogeneous treatment effects using random forests. *Journal of the American Statistical Association*, 113(523):1228–1242, 2018. doi: 10.1080/01621459.2017.1319839. URL <https://doi.org/10.1080/01621459.2017.1319839>.
- H. Wang and C.-L. Tsai. Tail index regression. *Journal of the American Statistical Association*, 104(487):1233–1240, 2009. doi: 10.1198/jasa.2009.tm08458. URL <https://doi.org/10.1198/jasa.2009.tm08458>.
- H. J. Wang and D. Li. Estimation of extreme conditional quantiles through power transformation. *American Statistical Association*, pages 1062 – 1074, 2013. doi: 10.1080/01621459.2013.820134. URL <https://doi.org/10.1080/01621459.2013.820134>.



- H. J. Wang, D. Li, and X. He. Estimation of high conditional quantiles for heavy-tailed distributions. *American Statistical Association*, pages 1453 – 1464, 2012. doi: 10.1080/01621459.2012.716382. URL <https://doi.org/10.1080/01621459.2012.716382>.
- S. Yang. Censored median regression using weighted empirical survival and hazard functions. *Journal of the American Statistical Association*, 94(445):137–145, 1999. doi: 10.1080/01621459.1999.10473830. URL <https://www.tandfonline.com/doi/abs/10.1080/01621459.1999.10473830>.
- B. D. Youngman. Generalized additive models for exceedances of high thresholds with an application to return level estimation for u.s. wind gusts. *Journal of the American Statistical Association*, 114(528):1865–1879, 2019. doi: 10.1080/01621459.2018.1529596. URL <https://doi.org/10.1080/01621459.2018.1529596>.
- K. Yu and M. C. Jones. Local linear quantile regression. *Journal of the American Statistical Association*, 93(441):228–237, 1998. doi: 10.1080/01621459.1998.10474104. URL <https://www.tandfonline.com/doi/abs/10.1080/01621459.1998.10474104>.
- K. Yu, Z. Lu, and J. Stander. Quantile regression: Applications and current research areas. *Journal of the Royal Statistical Society. Series D (The Statistician)*, 52(3):331–350, 2003. ISSN 00390526, 14679884. URL <http://www.jstor.org/stable/4128208>.